Evidence of silica leakage to the tropical Atlantic via Antarctic Intermediate Water during Marine Isotope Stage 4

James D. Griffiths[1*], Stephen Barker[1], Katharine R. Hendry[2§], David J. R. Thornalley[1§], Tina van de Flierdt[3], Robert F. Anderson[4], Ian R. Hall[1]

[1]School of Earth and Ocean Sciences, Cardiff University, Cardiff CF10 3AT, UK. e-mail: griffithsjd@cf.ac.uk (corresponding author), barkers3@cf.ac.uk, ThornalleyDJ@cf.ac.uk, Hall@cf.ac.uk. [2]Woods Hole Oceanographic Institution, Woods Hole MA 02543-1050, USA. e-mail:khendry@whoi.edu. [3]Department of Earth Science and Engineering, Imperial College London, London SW7 2AZ. e-mail: tina.vandeflierdt@imperial.ac.uk. [4] Lamont-Doherty Earth Observatory, P.O. Box 1000, 61 Route 9W, Palisades, NY 10964-1000, USA. e-mail:boba@ldeo.columbia.edu.

* Corresponding author

§ Now at the School of Earth and Ocean Sciences, Cardiff University, Cardiff, CF10 3AT, UK. e-mail: HendryKR@cf.ac.uk (KRH); and Woods Hole Oceanographic Institution, Woods Hole MA 02543-1050, USA. e-mail: dthornalley@whoi.edu (DJRT)

Abstract

Antarctic Intermediate Water (AAIW) and Subantarctic Mode Water (SAMW) are the main conduits for the supply of dissolved silica (silicic acid) from the deep Southern Ocean to the low latitude surface ocean, and therefore have an important control on low latitude diatom productivity. Enhanced supply of silicic acid by AAIW (and SAMW) during glacial periods may have enabled tropical diatoms to outcompete carbonate-producing phytoplankton, decreasing the relative export of inorganic to organic carbon to the deep ocean and lowering atmospheric CO_2. This mechanism is known as the 'Silicic Acid Leakage Hypothesis' (SALH). Here we present records of neodymium and silicon isotopes from the western tropical Atlantic that provide the first direct evidence of increased silicic acid leakage from the Southern Ocean to the tropical Atlantic within AAIW during glacial Marine Isotope Stage (MIS) 4 (~60-80 ka). This leakage is coeval with enhanced diatom export in the NW Atlantic and across the eastern equatorial Atlantic and provides support for the SALH as a contributor to CO_2 drawdown during full glacial development.

Main Text

Introduction

Pockets of the ancient atmosphere trapped in Antarctic ice cores show that the atmospheric concentration of CO_2 (pCO_2) was 80-100 ppmv lower during peak glacial times than the preindustrial Holocene value of ~ 280 ppmv [*Barnola et al.*, 1987; *Petit et al.*, 1999]. It is generally agreed that the causal mechanism for the glacial-interglacial (G-IG) pCO_2 change must be closely linked to the ocean carbon reservoir as this is the only active reservoir on Earth of sufficient size to account for the magnitude and frequency of the observed G-IG

cycles in pCO_2 [*Broecker*, 1982]. Many possible mechanisms have been proposed to explain all or part of the glacial decrease in pCO_2, which range from physical changes in ocean circulation [*Sarmiento and Toggweiler*, 1984] to biological processes [*Sarmiento and Toggweiler*, 1984; *Martin*, 1990] and the redistribution of carbonate sediment deposition [*Berger*, 1982]. It is generally thought though that the specific controls must be manifold [*Sigman et al.*, 2010].

Diatoms (unicellular algae) play a major role in the carbon, silica and nutrient budgets of the oceans [*Nelson et al.*, 1995; *Ragueneau et al.*, 2000], and may be important in regulating pCO_2 through their influence on the global biological pump that transports carbon from the surface to the deep ocean [*Ragueneau et al.*, 2000]. For example, changes in the relative contributions of silica versus carbonate secreting organisms in the surface ocean can influence pCO_2 by altering the ratio of organic to inorganic carbon exported to the deep sea [*Archer and Maier-Reimer*, 1994]. In the modern equatorial Atlantic, diatom growth is limited by the availability of silicic acid [$Si(OH)_4$] [*Nelson et al.*, 1995; *Sarmiento et al.*, 2004], which is the major nutrient required by diatoms to build their protective outer frustules. Under conditions of plentiful silica in surface waters, diatoms are often able to dominate primary productivity [*Ragueneau et al.*, 2000]. Mesocosm experiments conducted with semi-continuous nutrient addition show that diatoms are able to outcompete the commonly occurring calcareous coccolithophore *Emiliana huxleyi* and other picoplankton when concentrations of $Si(OH)_4$ are greater than ~2 μM and phosphate (PO_4^{3-}) and nitrate (NO_3^-) are present in non-limiting concentrations [*Egge and Aksnes*, 1992]. Changes in the supply ratio of $Si(OH)_4$ to NO_3^- to the surface of the equatorial Atlantic might then be expected to influence the ratio of silica to carbonate producers in this region [*Brzezinski et al.*, 2002; *Matsumoto et al.*, 2002].

69 The supply of nutrients to the low latitude Atlantic thermocline is determined by the
70 flux and preformed chemistry of AAIW and SAMW spreading north from their formation
71 regions within the Southern Ocean [*Sarmiento et al.*, 2004]. AAIW forms through the
72 subduction near the Polar Front (PF) of waters originating from the Winter Water (WW)
73 layer of the Bellingshausen Sea to the west of the Antarctic Peninsula [*Sievers and Nowlin*,
74 1984; *Meredith et al.*, 1999]. SAMW is a pycnostad (layer of near-uniform density), which
75 forms a circumpolar belt that encompasses the Subantarctic Zone (SAZ), between the
76 Subtropical Front (40-45 °S) and the Subantarctic Front (45-55°S), as well as the PF
77 [*Sarmiento et al.,* 2004; *Aoki et al.*, 2007]. SAMW has a relatively low silica content with
78 respect to other nutrients such as nitrate and phosphate, due to depletion of silicic acid by
79 diatoms (Figure 2). It has been proposed that the densest varieties of SAMW transit the Drake
80 Passage and contribute to AAIW in the Atlantic [*McCartney*, 1977; *Hanawa and Talley*,
81 2001]. The influence of AAIW at lower latitudes has been documented by its presence as a
82 silica maximum along an isopycnal (σ_0 ~27.4-27.6 kg m^{-3}) from 50°S to the Straits of Florida,
83 via the north coast of South America, the Caribbean Sea and the Yucatan Channel; and from
84 here extending northward to Cape Hatteras, and as far northeast to 60°N, 20°W, just south of
85 Iceland [*Tsuchiya*, 1989].

86 Southern Ocean (SO) surface waters are sourced from Upper Circumpolar Deep
87 Water (UCDW), which upwells south of the Antarctic Polar Front (APF) and has a relatively
88 high silica:nitrate ratio (Si:N ≈ 2 to 3) [*Schlitzer*, 2000]. As a result, primary productivity in
89 Antarctic Surface Water (AASW) is dominated by diatoms. Furthermore, diatoms in this
90 region take up 4-5 times as much silica per unit of organic matter than those from other
91 regions of the world ocean [*Pondaven et al.*, 2000; *Brzezinski et al.*, 2001]. This is due partly
92 to the fact that the Southern Ocean is iron-limited, which increases the uptake of silica

93 relative to nitrate in diatoms [*Takeda*, 1998]. This process leaves AASW depleted in $Si(OH)_4$,
94 but high in preformed NO_3 and PO_4 [*Schlitzer*, 2000] (Figure 1).

95 If the silica uptake of diatoms in surface waters of the Southern Ocean were to be
96 decreased (for example by an increase the supply of Fe), then any unused silicic acid would
97 'leak' to lower latitudes via AAIW (provided that it was not completely consumed by
98 diatoms in the Subantarctic Zone) [*Matsumoto et al.*, 2002]. Higher concentrations of silicic
99 acid, conveyed to low latitudes by AAIW, could alleviate Si limitation there, allowing
100 diatoms to increase their contribution to primary productivity, and potentially outcompete
101 carbonate-producers such as coccolithophorids [*Brzezinski et al.*, 2002; *Matsumoto et al.*,
102 2002]. The net result of such an ecological shift would be that pCO_2 is drawn down through a
103 combination of changes in surface- and whole-ocean alkalinity [*Matsumoto et al.*, 2002;
104 *Matsumoto and Sarmiento*, 2008]. This mechanism is known as the Silicic Acid Leakage
105 Hypothesis (SALH).

106 Here we test the SALH during the development of full glacial conditions at the MIS
107 5/4 boundary by producing records of authigenic (seawater-derived) neodymium (Nd)
108 isotopes, expressed as ε_{Nd} [$\varepsilon_{Nd} = (^{143}Nd/^{144}Nd_{sample}/^{143}Nd/^{144}Nd_{CHUR} - 1)*10000$); CHUR =
109 chondritic uniform reservoir = 0.512638, [*Jacobsen and Wasserburg*, 1980] and sponge
110 spicule silicon (Si) isotopes, expressed as $\delta^{30}Si$ [$\delta^{30}Si = [[(^{30}Si/^{28}Si)_{sample}/(^{30}Si/^{28}Si)_{standard}] - 1]$
111 x 10^3)]; from a sediment core retrieved from the Tobago Basin (MD99-2198; 12.09°N;
112 61.23°W; 1330m water depth). The core site is currently bathed by AAIW (Figure 1)
113 [*Schlitzer*, 2000]. The Nd isotope record provides an indication of the relative influences of
114 intermediate waters sourced from northern versus southern high latitudes in the tropical
115 Atlantic [*Pahnke et al.*, 2008] while the silicon isotopes give information about changes in
116 intermediate water $Si(OH)_4$ at our core site [*Hendry et al.*, 2010; *Hendry and Robinson*,
117 2012]. We also measured percent sedimentary opal in MD99-2198, and (thorium-normalised)

sedimentary opal accumulation rates in Bermuda Rise core ODP 1063 (33°41'N; 57°37'W; 4595 m water depth) and eastern equatorial Atlantic core RC24-01 (0°33'N, 13°39'W; 3837m water depth) to gauge any effect on low-latitude diatom export productivity during the MIS 5/4 transition. In particular, we test whether a SALH scenario could have played a role in the ~46 ppmv drawdown of pCO_2 that occurred ~ 72 ka, at the initiation of MIS 4 [*Ahn and Brook*, 2008], as a number of cores from the eastern equatorial Atlantic (EEA) indicate increased opal accumulation during MIS 4 [*Gardner and Burckle*, 1975; *Stabell*, 1986; *Abrantes*, 2001].

Core Locations and Hydrography

MD99-2198 (12.09˚N; 61.23˚W; 1330 m water depth) is situated in the Tobago Basin in the south eastern sector of the Caribbean Sea (Figure 2). Caribbean Sea surface waters (0-80 m) are nutrient-depleted and are underlain by high-salinity Subtropical Under Water (SUW) between ~80-100 m. Below this, a mixture of SUW and AAIW forms the main component of Caribbean thermocline waters present at depths ~500-900 m. The composition of intermediate waters at this site (termed Atlantic Intermediate Water - AIW, at depths ~900-1900 m) is a mixture of AAIW and Upper North Atlantic Deep Water (UNADW). UNADW dominates below 1900 m [*Wüst*, 1964; *Haddad and Droxler*, 1996].

AAIW enters the Tobago Basin via the subthermocline North Brazil Current (NBC), which contains approximately 60 ± 5% southern-sourced water [*Bub and Brown*, 1996]. Depending on the season, all or a part of these southern-sourced waters retroflect anticyclonically and flow eastwards, feeding into the North Equatorial Undercurrent (NEUC) [*Wilson et al.*, 1994; *Suga and Talley*, 1995]. North Atlantic Central Water (NACW) enters the region between the equator and 9°N and west of 44°W, and mixes with the southern-

142 sourced water. This mixed water mass makes up approximately half of the region in volume
143 and is predominantly of a southern origin [*Bub and Brown*, 1996].

144 The ODP core site 1063 (33°41'N; 57°37'W; 4595 m water depth) is situated on the
145 Bermuda Rise, an area of very high sediment accumulation, mainly sourced from Canadian
146 rivers [*Laine and Hollister*, 1981] (Figure 2). Sediments on the north side of the Bermuda
147 Rise are resuspended by the Gulf Stream and deep recirculating gyres [*Laine and Hollister*,
148 1981]. Primary productivity is low due to the oligotrophic surface waters bounded by the
149 North Atlantic Subtropical Gyre (NASG), and modern biogenic silica production rates are
150 amongst some of the lowest in the world ocean [*Brzezinski and Nelson*, 1995; *Nelson and*
151 *Brzezinski*, 1997].

152 We also generated opal flux records from the core RC24-01 (0˚33'N; 13˚39'W; 3837
153 m water depth), situated in the EEA (Figure 2). The RC24-01 core site lies in the divergence
154 created by the boundaries of the broad, westward-flowing South Equatorial Current (SEC)
155 and the weaker, more variable eastward-flowing Northern Equatorial Counter Current
156 (NECC) [*Bourles et al.*, 1999; *Stramma and Schott*, 1999]. Silicate and salinity profiles
157 demonstrate that AAIW is present as a layer in the EEA at depths of 800-1000m [*Schlitzer*,
158 2000]. In the modern ocean AAIW influences the EEA after flowing eastward from the NBC
159 at 3 - 4°S of the equator and also more weakly at 1 - 2°N [*Suga and Talley*, 1995].

160

161 *Methods*

162 Neodymium isotope ratios were measured on the dispersed Fe-Mn oxyhydroxide phase
163 extracted from the fine (<63 μm) fraction of the de-carbonated bulk sediment from MD99-
164 2198 sediment samples. In detail, the <63μm fraction of the sample (~4cm^3 bulk) was

separated out by wet sieving. All carbonate was removed from the sample using buffered glacial acetic acid, until no signs of a reaction were detectable. Fe-Mn oxides were subsequently extracted using a 0.02 M solution of hydroxylamine hydrochloride (HH) for 2 hours, after [*Chester and Hughes*, 1967]. After drying down the solution at a high temperature to destroy the HH, the samples were redissolved in 3M HNO_3^- for two-stage ion chromatography. Separation of rare earth elements (REE) from the sample matrix was achieved using TRU-spec resin, and separation of Nd from the other REE was achieved using Ln-spec resin. Neodymium isotopes were measured in static mode on a Nu Plasma Multi-Collector Inductively-Coupled Plasma Mass Spectrometer (MC-ICP-MS) in the MAGIC laboratories at Imperial College London. Mass bias correction was accomplished using a $^{146}Nd/^{144}Nd$ ratio of 0.7219. During the course of the sample analyses (3 separate days) JNd_i standards yielded $^{143}Nd/^{144}Nd$ values of 0.512105 ± 0.000017 (2σSD, n=21) , 0.512112 ± 0.000012 (2σ SD, n=14), and 0.512057 ± 0.000015 (2σ SD, n=19), respectively. All sample values were normalised to the recommended JNd_i $^{143}Nd/^{144}Nd$ ratio of 0.512115 [*Tanaka et al.*, 2000] (see Table 1).

Sponge spicules were picked from the 63-215μm fraction of the previously-separated coarse (<63μm) fraction of MD99-2198. The species from which the spicules came were not identified as previous work had suggested that the species of sponge does not affect the relationship between $[Si(OH)_4]$ and $\delta^{30}Si$ [*Hendry et al.*, 2010].

The sponge spicules were cleaned in H_2O_2, and dissolved in 0.4 M NaOH at 100°C for three days. The solutions were then diluted and acidified to pH~2-3. A cation exchange resin (BioRad AG50W-X12) was used to quantitatively separate Si from other major ions [*Georg et al.*, 2006]. Si isotopes were measured on a Thermo Neptune Multi-Collector Inductively Coupled Plasma Mass Spectrometer at Woods Hole Oceanographic Institution. Full operating conditions are described in [*Hendry et al.*, 2010]. Solutions were run at least in

duplicate by both standard-sample bracketing and bracketing with Mg-doping, whereby samples and bracketing standards were spiked with Mg standard (Inorganic Ventures), and intensity-matched for ^{28}Si and ^{24}Mg signals within 10% (typically within 5%). The $^{29}Si/^{28}Si$ isotope ratios were corrected using a fractionation factor calculated using the measured $^{25}Mg/^{24}Mg$ ratios, see [*Cardinal et al.*, 2003] for details. Repeat analyses of an opal standard LMG08 [*Hendry et al*., 2011] measured by standard-sample bracketing of an opal standard over a period of several months yields values of -1.75 ± 0.1‰ for $\delta^{29}Si$ and -3.43 ± 0.23‰ (2SD) for $\delta^{30}Si$, providing the most conservative estimate of uncertainty, see Table 2.

Concentrations of protactinium (^{231}Pa), thorium (^{230}Th, ^{232}Th), and uranium (^{234}U and ^{238}U) in RC24-01 were determined at Lamont-Doherty Earth Observatory (L-DEO), according to the method of [*Anderson and Fleer*, 1982; *Fleisher and Anderson*, 2003]. Approximately 0.1g of bulk sediment was digested using HNO_3^-, $HClO_4$ and HF. Anion resin column chemistry was then used to separate out the Pa and U/Th fractions. The concentration of each radionuclide species was then measured using a VG Axiom Multi-Collector Inductively-Coupled Plasma Mass Spectrometer. The Pa isotopes were measured in 'Flight Tube Scan Mode', and only monitored the masses 231 and 233. Precision on the 231/233 ratio was better than 2.5% at the 1 sigma level, for 5 replicates. See [*Fleisher and Anderson*, 2003] for full operating conditions. Authigenic uranium (U_{auth}) was determined from the concentrations of ^{232}Th and ^{238}U, assuming a detrital ^{232}Th contribution of 10ppm [*Bradtmiller et al.*, 2007]. To account for sedimentary redistribution, we normalised the sedimentary opal content to the flux rate of ^{230}Th, to produce a record of opal flux [*Bacon*, 1984; *Francois et al.*, 2004]. Opal flux was calculated as follows: 0.01 x ^{230}Th-norm F x % opal (see Table 3 for data). Opal was measured in all cores using ~100mg of bulk sediment. Sedimentary opal content was measured using the wet alkaline extraction method of [*Mortlock and Froelich*, 1989].

215

216 *Core Age Control*

217 The North Greenland Ice Core Project (NGRIP) $\delta^{18}O$ record was used as a basis for
218 all core age models used in this study. The NGRIP $\delta^{18}O$ is on the Greenland Ice Core
219 Chronology 2005 (GICC05) age model back to 60 ka [*Andersen et al.*, 2007]. Between 60
220 and 100 ka the NGRIP $\delta^{18}O$ record has been tuned to the $\delta^{18}O$ record from Chinese
221 speleothems [*Thornalley et al.,* 2012, submitted ms], based on the observed in-phase
222 relationship between the speleothem records and Greenland temperature during MIS 3 [*Wang*
223 *et al.*, 2001; *Wang et al.*, 2008].

224 Age control for MD99-2198 (Figure 3) was derived by tuning its record of planktic
225 foraminiferal $\delta^{18}O$ (*Globigerinoides ruber*, white, picked from 250-315 μm of the coarse
226 fraction) to NGRIP $\delta^{18}O$. This approach assumes in-phase behaviour between millennial-
227 scale oscillations in the tropics and the northern hemisphere temperature. We suggest that this
228 is reasonable, because these regions are linked through meridional heat transport and the
229 position of the Intertropical Convergence Zone (ITCZ) (which is sensitive to changes in
230 North Atlantic temperature) [*Hüls and Zahn*, 2000; *Peterson et al.*, 2000; *Lea et al.*, 2003;
231 *Cruz et al.*, 2005]. It has also been demonstrated that the primary control on the $\delta^{18}O$ of
232 rainfall over tropical South America is the amount of precipitation, which is modulated by the
233 position of the ITCZ [*Vuille et al.*, 2003; *Cruz et al.*, 2005].

234 The L* reflectance index (a measure of sediment brightness) may be used to
235 distinguish sedimentological components such as free and bound Fe, $CaCO_3$, Fe-minerals
236 (e.g. goethite), and clay [*Rogerson et al.*, 2006]. A high-resolution record of core reflectance
237 (similar to L*) from the western tropical Atlantic was used to identify a link between
238 sediment reflectance changes in the Cariaco Basin (northern coastal Venezuela) to Greenland

239 ice core $\delta^{18}O$ changes, thereby demonstrating a clear linkage of the tropical hydrological
240 cycle with high northern latitude climate [*Peterson et al.*, 2000]. In light of this finding, the
241 L* index of MD99-2198 [*Hüls and Zahn*, 2000] can be used to provide additional support for
242 the NGRIP-tuned age model of MD99-2198 (Figure 3).

243 ODP 1063 age control was obtained by tuning core reflectance and magnetic
244 susceptibility to records of orbital precession and obliquity [*Grützner et al.*, 2002], and
245 further refined by tuning the planktic $\delta^{18}O$ record (*Globorotalia inflata*) to NGRIP $\delta^{18}O$
246 [*Thornalley et al.,* 2012, submitted ms]. Age control for RC24-01 was derived by tuning its
247 record of % $CaCO_3$ to that of ODP 1063 [*Thornalley et al.,* 2012, submitted ms] (Figure 4).
248 The $CaCO_3$ record in RC24-01 is thought to relate to millennial-scale oscillations in northern
249 hemisphere climate and changes in deepwater chemistry [*Sarnthein et al.*, 1994; *Sarnthein et*
250 *al.*, 2000], therefore we suggest that it is reasonable to link the changes in the $CaCO_3$ content
251 of RC24-01 with those in ODP 1063.

252

253 *Results and Discussion*

254 Porewater profiles of Rare Earth Elements (REEs) from marine pelagic sediments
255 demonstrate that under oxic to suboxic conditions trace metals such as Nd are scavenged
256 from seawater and incorporated into Fe-Mn oxyhydroxide coatings in the uppermost few
257 centimetres of sediment [*Haley et al.*, 2004]. This observation has been exploited in a number
258 of studies to reconstruct seawater Nd isotopic compositions using such dispersed Fe-Mn
259 hydroxide coatings, for example [e.g., *Rutberg et al.*, 2000; *Bayon et al.*, 2002; *Piotrowski et*
260 *al., 2004, 2005; Gutjahr et al.*, 2007; *Gutjahr et al.*, 2008; *Pahnke et al.*, 2008].

Extracting the authigenic Nd signal from oxyhydroxide coatings by sequential leaching, Pahnke et al. (2008) found that the core top value of MD99-2198 agreed within one epsilon unit with the seawater Nd isotopic compositions from stations near the Tobago Basin [*Piepgras and Wasserburg*, 1987], even though strontium (Sr) isotopes measured on the same leachates deviated significantly from seawater. This observation confirms the mass balance calculations by Gutjahr et al. (2007), implying that even in cases of significant detrital contamination of the Sr isotope signal, Nd isotopes can still preserve an authigenic signature. We used exactly the same leaching protocol as Pahnke et al. (2008), providing confidence that Fe-Mn leachate results of bulk sediments at this site yield robust authigenic Nd isotopic compositions.

Seawater Nd isotopes across the MIS 5/4 transition from MD99-2198 show a range in ε_{Nd} from -9.1 to -11.0 (Figure 5, red curve c). Relatively unradiogenic values (ε_{Nd} = -10 to -11) are displayed during the latter part of MIS 5, which suggest a significant influence of Northern Component Water (NCW) on the western tropical Atlantic during MIS 5a. These values are furthermore similar to the core top value of -11 [*Pahnke et al.,* 2008], which reflects modern mixing of NADW with a typical ε_{Nd} = -13 to -14 [*Piepgras and Wasserburg*, 1987; *Lacan and Jeandel*, 2005] with a smaller proportion of more radiogenic AAIW [ε_{Nd} = -7 to -9 [Piepgras and Wasserburg, 1982; Jeandel, 1993; Stichel et al., 2012].

During MIS 4, our record shows an abrupt change to a less negative (more radiogenic) ε_{Nd}, beginning at ~69 ka, and reaching a maximum at ~65 ka. Subsequently the ε_{Nd} values decrease between 65 and 63 ka, suggesting a slight enhancement of NCW influence. The lowest value attained at ~65 ka is ε_{Nd} = -9.1, which is approaching the South Atlantic/AAIW endmember.

The $\delta^{30}Si$ data (Figure 6, blue curve d) obtained in this study are interpreted to reflect changes in the ambient silicic acid concentration of AAIW using the relationship in Equation 1 (below) [*Hendry and Robinson*, 2012], assuming a seawater $\delta^{30}Si$ value of +1.5 ± 0.07 ‰ (2 standard error) [*de Souza et al.*, 2012]:

$$(1) \qquad [Si(OH)_4] = (270/\Delta^{30}Si + 6.54)) - 53 \qquad (R^2 = 0.83)$$

Where $\Delta\delta^{30}Si = \delta^{30}Si_{sponge} - \delta^{30}Si_{seawater}$. Assuming that $\delta^{30}Si_{seawater}$ remained within the range +1.5 to 2‰ within the interval of interest (compared to a modern value of +1.5‰ ± 0.07, 2 standard error) [*de Souza et al.*, 2012]. Whilst the possibility exists that the silicon isotope composition ($\delta^{30}Si(OH)_4$) of AAIW may not have been the same as in the modern ocean due to differences in silica input, we considered this scenario unlikely for two reasons. Firstly, the range in silicic acid concentration (and the silicon isotope composition) in modern AAIW is small, ~ 1.5-1.8 ‰ [*Cardinal et al.,* 2005*; Hendry et al.*, 2010; *de Souza et al.*, 2012] compared to that in sponges [*Hendry and Robinson*, 2012]. Given this variability, we plot the possible range of silicic acid concentrations (shaded orange area in Figure 6).

Secondly, we infer a major change in the silicic acid content of AAIW over a timescale <10 ka, which is of the same order as the oceanic residence time of dissolved silica, estimated at ~10-15 ka [*Tréguer et al.*, 1995; *Georg et al.,* 2009]. We therefore suggest that even large changes in silica input to the oceanic reservoir could not alter its silicon isotope composition significantly over the timescale of our record.

Our results suggest an increase in ambient [$Si(OH)_4$] of ~15 to 20 μM between MIS 5a and 4 (Figure 6). This increase would probably have been sufficient to alleviate Si limitation on low-latitude diatom production [*Egge and Aksnes*, 1992].

The changes in $\delta^{30}Si$ across MIS 5/4 in the MD99-2198 record are small compared to the range measured by Hendry and Robinson (2012) in different parts of the world ocean, and are subject to large uncertainty relative to their range (see Figure 6). However, the fact that inferred silicic acid concentrations increase into MIS 4, when Nd isotopes suggest an increase in southern component water, implies a leakage of high-silica intermediate water of a southern origin during MIS 4.

Silicic acid leakage during MIS 4 appears to have had no effect on the diatom export productivity at the MD99-2198 core site (purple curve f, Figure 5). However, the record of percent opal from ODP 1063 (purple curve g, Figure 5) demonstrates a sustained increase within MIS 4. The records of percent opal (purple curve h, Figure 5) and thorium-normalised opal flux (brown curve i, Figure 6) from RC24-01 also reveal an increase during MIS 4.

The relationship between the silicic acid content of AAIW, as inferred from the $\delta^{30}Si$ record from the Tobago Basin and low latitude diatom productivity is not straightforward. However, the data does appear to support the SALH, in that a more sustained increase in opal occurs contemporaneously with the most negative $\delta^{30}Si$ values during MIS 4 (equivalent to the highest silicic acid concentrations). The correspondence of the initiation of changes within both records, and maximum values in MIS 4 suggests some common control on both records.

328 *Discussion of oceanographic changes MIS 5a/4*

329 The records of ε_{Nd} and $\delta^{30}Si$ from MD99-2198 (Figure 5) suggest a major re-
330 organisation in the low-latitude oceans at the MIS 5/4 transition. The ε_{Nd} during MIS 5a is -
331 10 to -11, similar to modern values, and is analogous to the modern scenario of Atlantic
332 Intermediate Water (AIW), a combination of AAIW and Upper North Atlantic Deep Water
333 (UNADW) [*Wüst*, 1964; *Haddad and Droxler*, 1996], bathing the MD99-2198 core site. The
334 reconstruction of ε_{Nd} in MIS 5a further implies that some variety of northern component
335 water (NCW), with a similar Nd isotopic signature to modern NADW, was influencing the
336 mid depth western tropical Atlantic in this interval. This inference is in agreement with
337 studies from several locations in the Atlantic, using sedimentary $_{xs}(^{231}Pa/^{230}Th)_0$ as an
338 indicator of the strength of Atlantic Meridional Overturning Circulation (AMOC) changes as
339 well as ε_{Nd} [*Rutberg et al.*, 2000; *Piotrowski et al.*, 2005; *Guihou et al.*, 2010].

340 In order to understand the ε_{Nd} record generated from MD99-2198 we considered the
341 potential effect that other water masses could have had on the Nd isotopic record at our core
342 site. Southern and western Indian Ocean intermediate and deep waters have $\varepsilon_{Nd} \approx$ -7 to -9
343 (reflecting dominance of northward flowing circumpolar water) [*Piepgras and Wasserburg*,
344 1982; *Bertram and Elderfield*, 1993; *Jeandel*, 1993; *Jeandel et al.*, 1998; *Stichel et al.*, 2012],
345 which are similar to the Nd isotopic composition of AAIW. Deep and intermediate waters
346 from the Indian Ocean therefore have the potential to have influenced the intermediate depth
347 Tobago Basin and contributed to the more radiogenic values of ε_{Nd} recorded during MIS 4. A
348 major mechanism for the exchange of heat and salt in surface and intermediate waters
349 between the Indian Ocean and the South Atlantic is the intermittent shedding of large-scale
350 rings, filaments and eddies of Indian Ocean water from the Agulhas current and retroflection
351 off South Africa [*de Ruijter et al.*, 1999]. We suggest that Agulhas leakage is unlikely to have
352 influenced the Nd isotopic record of MD99-2198, as a study of the exchange of heat and salt

353 between the Atlantic and Indian Oceans via the Agulhas retroflection suggests that the input
354 of Indian Ocean water into the South Atlantic was relatively minor during MIS 4 [*Peeters et*
355 *al.*, 2004]. However, more recent results question the presumption of reduced Agulhas
356 leakage during glacial periods [*Martínez-Méndez et al.*, 2010], and so the influence of Indian
357 Ocean water on the western tropical Atlantic remains difficult to constrain, and cannot be
358 ruled out entirely as an influence on the MD99-2198 Nd isotopic record.

359 Another water mass that may have influenced the hydrography and hence the Nd
360 isotopic composition in the Tobago Basin during MIS 5/4 is Mediterranean Overflow Water
361 (MOW). Modern MOW at the outflow from the Strait of Gibraltar is characterised by a ε_{Nd} of
362 ≈ -9.5 [*Tachikawa et al.*, 2004], a value within error of the maximum ε_{Nd} recorded during
363 MIS 4 in MD99-2198. The net flux of MOW in to the North Atlantic was lower in MIS 2
364 than during northern hemisphere stadials and Heinrich events [*Voelker et al.*, 2006], and
365 therefore was probably low during MIS 4, but cannot be fully excluded as a potential
366 contributor to the Nd isotopic excursion recorded during MIS 4 in MD99-2198.

367 Besides considering the effect changes in volume (and hence mixing proportions) of
368 water masses in the Tobago basin have on seawater Nd isotopes, it is also possible for
369 vertical changes in water mass boundaries to have had an influence [*R. Xie, personal*
370 *communication*]. MD99-2198 lies at the lower limit of modern AAIW (1330m, see Figure 2),
371 and may therefore be sensitive to changes in the depth of the boundary between AAIW and
372 Glacial North Atlantic Intermediate Water (GNAIW), a glacial analogue of NADW [*Oppo*
373 *and Lehman*, 1993]. If AAIW shoaled to ~1000 metres during glacial periods, as predicted to
374 have occurred in the Last Glacial Maximum (LGM) [*Curry and Oppo*, 2005], or was absent,
375 the MD99-2198 core site would have been bathed by GNAIW [*Curry and Oppo*, 2005;
376 *Marchitto and Broecker*, 2006]. However, GNAIW probably had a similar Nd isotopic
377 signature to modern NADW [*van de Flierdt et al.*, 2006; *Foster et al.*, 2007], and therefore

would result in a shift to lower ε_{Nd} values during MIS 4, which is contrary to the higher values observed in MD99-2198 during MIS 4. Hence, we discount shoaling of the AAIW-GNAIW boundary as an influence on our Nd isotopic record.

One last point for consideration is our implicit assumption of stability in the Nd isotopic compositions of the source region of southern water masses. This assumption may, however, be compromised by the fact that decreased export of NADW/GNAIW to the Southern Ocean will have an effect on the Nd isotopic composition of water masses formed in the Southern Ocean. Data extracted from a deep-sea coral skeleton from the Drake Passage indicate that intermediate waters during Heinrich Stadial (HS) 1 (~16.7 ka) became more radiogenic [*Robinson and van de Flierdt*, 2009], probably due to reduced input of North Atlantic-sourced Nd to the Drake Passage, associated with decreased NADW export [*Keigwin et al.*, 1994; *McManus et al.*, 2004] resulting in more 'Pacific-like' values in the Southern Ocean. It remains to be seen whether a similar scenario could have made the Nd isotopic composition of SAMW and AAIW source regions more radiogenic during MIS 4. Heinrich Stadials are considered times of most pronounced changes in ocean circulation [*Keigwin et al*., 1994; *McManus et al.*, 2004] and hence we render similar magnitude changes in seawater Nd isotopes in the Southern Ocean during MIS 4 less likely. While we cannot fully exclude that the ε_{Nd} excursion recorded during MIS 4 was a result of decreased NADW export, our preferred interpretation is that elevated values reflect increased influence of AAIW in the Tobago Basin.

The results of this study take on more significance when they are examined alongside the Si isotope data. The correlation ($r = -0.7$ at $p < 0.05$) between the Nd isotopic record and the silicon isotopic record of silicic acid concentrations in MD99-2198 (Figure 5) imply that the water's origin was in the subantarctic zone (~100μM of silicic acid) [*Schlitzer*, 2000]

because the mid- and northern Atlantic is depleted in silicic acid due to depletion by diatoms in subtropical anticyclonic gyre systems [*Levitus et al.*, 1993]. The only region of the ocean that contains sufficient silicic acid to affect a significant change in the silicic acid content of AAIW is the deep SO [*Schlitzer*, 2000].

The most important sources of dissolved silica to the ocean are rivers [*Tréguer et al.*, 1995], which must also be considered as potential suppliers of silicic acid to the Tobago Basin during MIS 4. The modern eastern Caribbean Sea is influenced by freshwater input from both the Orinoco River [*Chérubin and Richardson*, 2007] and the Amazon River [*Chérubin and Richardson*, 2007; *Molleri et al.*, 2010]. However, input of sediment to the eastern Caribbean during glacial periods is likely to have been lower from the Amazon River, due to decreased rainfall over South America because of a southward shift in the position of the ITCZ [*Peterson and Haug*, 2006]. Moreover, Amazon plume waters become quickly depleted in silica due to high productivity by siliceous phytoplankton in the Amazon shelf waters [*DeMaster et al.*, 1996].

However, sedimentary input from the Orinoco River may have been higher [*Bowles and Fleischer*, 1985] because despite the fact that Orinoco outflow is also modulated by the position of the ITCZ, the proximity of the Aves Ridge to the Orinoco plume may cause volumetric increases in Orinoco River water during glacial lowstand [*Bowles and Fleischer*, 1985]. On the other hand, other evidence suggests that Orinoco River water is not a significant contributor of dissolved silica to the Tobago Basin; firstly, Orinoco River water generally contains low concentrations of dissolved and suspended constituents due to a high runoff [*Lewis and Saunders*, 1989]. More importantly, sediments from the lower Orinoco River display a less radiogenic Nd isotopic composition ($\varepsilon_{Nd} \sim -14$) [*Goldstein et al.*, 1997], relative to Amazon River sediments ($\varepsilon_{Nd} \sim -9.2$) [*Goldstein et al.*, 1984], which presumably would have made ε_{Nd} values during MIS 4 less radiogenic than those recorded in this study.

During MIS 5a, values of $\delta^{30}Si$ suggest that the silicic acid content of AAIW could have been at trace levels at the MD99-2198 core site. The silicic acid content of North Atlantic surface and intermediate waters is generally far lower than in the Southern Ocean [*Schlitzer*, 2000]. The combination of this observation with more negative ε_{Nd} during MIS 5a makes it far more likely that lower-silica NCW was a more dominant influence at intermediate depths in the western tropical Atlantic in this period, which is in agreement with the interglacial mode of tropical water mass circulation inferred from studies using other water mass tracers [*Curry and Oppo*, 2005; *Marchitto and Broecker*, 2006].

The apparent increase in silicic acid concentration observed during MIS 4 in MD99-2198 leads us to question whether the inferred changes in silicic acid concentration are due to an increase in the volumetric contribution of AAIW to the Tobago Basin, or to an increase in its preformed silicic acid concentration, or both. Records of the $\delta^{30}Si$ of diatoms from the Atlantic sector of the SO show more depleted $\delta^{30}Si$ values during MIS 4, which has been interpreted as an indication of lower silicic acid utilisation by diatoms in the Atlantic SO, and an increase in the silicic acid content of SO surface waters by corollary [*Brzezinski et al.*, 2002]. This lends support to the argument for an increased silicic acid content of AAIW during MIS 4.

A study of $\delta^{13}C$ in benthic foraminifera from the southeast Pacific (east of New Zealand) suggested lower glacial formation rates of AAIW for the past three G-IG cycles [*Pahnke and Zahn*, 2005; *Crosta et al.*, 2007]. However, Pahnke and Zahn (2005) also acknowledge that similar glacial excursions in benthic $\delta^{13}C$ could have been produced by upward displacement of the boundary between AAIW, and Upper Circumpolar Deep Water (UCDW), which exhibits more depleted glacial $\delta^{13}C$ values [*Hodell et al.*, 2003].

Spatial displacement of the AAIW-UCDW boundary is consistent with the inferred movement of westerly wind belts equatorward during glacial periods [*Toggweiler et al.*, 2006]. Additionally, positive $\delta^{13}C$ excursions interpreted by Pahnke and Zahn as periods of enhanced AAIW formation, are correlated with periods of enhanced upwelling inferred from increased opal fluxes, recorded near the APF in the Atlantic sector of the SO [*Anderson et al.*, 2009]. A more southerly position of the westerly wind belt increases upwelling whilst simultaneously displacing the AAIW-UCDW boundary southward and downward near the core site used in the Pahnke and Zahn study. Furthermore, a number of benthic $\delta^{13}C$ records from various depths around New Zealand support the notion of displacement of the AAIW-UCDW boundary [*Elmore et al.*, 2011]. Whilst the debate surrounding AAIW formation rates remains unresolved, we argue that there is no inconsistency between our inference of increased AAIW expression in the mid-depth western tropical Atlantic during MIS 4, and the benthic $\delta^{13}C$ record of Pahnke and Zahn (2005).

Increased levels of silicic acid at intermediate depths in the low latitude ocean would only have been able to relieve Si-limitation in the surface ocean if they had been able to reach the euphotic zone. Elevated silicic acid in AAIW influencing the mid-depth western tropical Atlantic during MIS 4 appears to have been unable to reach the euphotic zone there, and was therefore prevented from promoting greater diatom export productivity in the Tobago Basin, based on the opal record from MD99-2198 (Figure 5, purple curve f). A lack of upwelling in this interval may have been related to the depth of the western Atlantic thermocline, which is thought to have deepened throughout MIS 4 [*Rühlemann et al.*, 1996; *Höll et al.*, 1999].

Conversely, in the EEA, the thermocline appears to have been shallower than it was in the western Atlantic during MIS 4 [*Abrantes*, 2000; *Flores et al.*, 2000], due to enhanced northeast trade wind strength [*Flores et al.*, 2000; *Abrantes*, 2003] and greater rates of upwelling [*Jansen et al.*, 1996; *Abrantes*, 2000]. This might explain why leaked silicic acid

475 during MIS 4 may have been able to influence diatom export productivity in the EEA but not
476 the western equatorial Atlantic. The increase in opal observed in RC24-01 is aligned with
477 maxima in a range of palaeoproductivity proxies (Figure 7), as well as opal maxima in other
478 cores from across the EEA [*Gardner and Burckle*, 1975; *Stabell*, 1986; *Abrantes*, 2001]. This
479 strongly implies that the increase in opal accumulation during MIS 4 was a result of enhanced
480 diatom export productivity rather than enhanced opal preservation. Authigenic uranium
481 (U_{auth}) has been used as a proxy for organic carbon flux [*Kumar et al.*, 1995; *Anderson et al.*,
482 1998; *Chase et al.*, 2001] and provides support for the interpretation of an enhanced organic
483 carbon flux during MIS 4 from the F(TOC) record of RC24-01 (Figure 7, green curve c).
484 Additionally, the interpretation of an overall enhancement in export productivity during MIS
485 4 is consistent with a palaeoproductivity reconstruction using organic carbon and planktic
486 foraminiferal transfer functions from a core taken from the EEA [*Sarnthein et al.*, 1992].

487 Despite the coincidence of the enrichment of the Atlantic thermocline with silica, and
488 the enhancement of low latitude opal export, the mechanism required to mix AAIW from
489 depths of 800-1000 metres into the euphotic zone (<200 metres) is as yet unidentified.
490 SAMW has also been identified as a major conduit for preformed nutrients to the low
491 latitudes [*Sarmiento et al.*, 2004], and has the potential to alleviate low latitude Si-limitation
492 of diatom productivity, presumably being more readily entrained into the euphotic zone. A
493 recent ocean circulation experiment using the HYbrid isopycnic-cartesian Coordinate Ocean
494 general circulation Model (HYCOM) has demonstrated that SAMW-related tracer re-
495 emergence in the Atlantic at tropical latitudes may be strongly dependent on shear-induced
496 turbulent mixing, and furthermore that significant tracer re-emergence occurs in the North
497 Atlantic [*Zuo et al.*, 2012]. This latter finding may offer a possible explanation for the
498 increases in sedimentary opal in ODP 1063 recorded in this study. The study of SAMW
499 dynamics during glacial periods continues to be an interesting topic for future research.

500 The record of sedimentary opal from ODP 1063 (Bermuda Rise) is in line with results
501 from a number of cores from the EEA, in that it shows an increase in late MIS 4. We interpret
502 the record of % opal in ODP 1063 as reflecting increased diatom productivity at the Bermuda
503 Rise during MIS 4. This is consistent with other studies [*Keigwin and Boyle*, 2008; *Gil et al.*,
504 2009; *Lippold et al.*, 2009]. These findings imply that the northward penetration of AAIW
505 was enhanced relative to its modern extent [*Schlitzer*, 2000] during northern hemisphere
506 stadials and is also in agreement with the findings of [*Pahnke et al.*, 2008]. Today the
507 Bermuda Rise is a stratified, oligotrophic environment with low diatom productivity [*Heath*,
508 1974], but the site has witnessed significant increases in diatom productivity in the past
509 [*Keigwin and Boyle*, 2008; *Gil et al.*, 2009; *Lippold et al.*, 2009]. Processes such as cold-core
510 rings and mode-water eddies may have enabled silicic acid within AAIW/SAMW to be
511 brought into the euphotic zone, and therefore to have enhanced diatom productivity [‘*The*
512 *Ring Group’*, 1981; *Krause et al.*, 2009]. Melting icebergs are also thought to have had the
513 potential to affect diatom export productivity in waters overlying the Bermuda Rise, possibly
514 due to their amplification of cold-core rings [*Gil et al.*, 2009]. Additionally, increased glacial
515 eolian supply of Saharan dust to the Bermuda Rise [*Herwitz et al.*, 1996] and subsequent
516 dissolution of particulate silica [*Tréguer et al.*, 1995], cannot be excluded as an influence on
517 opal accumulation in ODP 1063, particularly as aeolian Fe appears to be important in co-
518 limitation of diatom growth [*Timmermans et al.*, 2004; *Brzezinski et al.*, 2011]. Nonetheless,
519 the coincidence of large increases in diatom productivity in oligotrophic areas of the ocean
520 with our new evidence for silicic acid leakage from high southern latitudes is compelling, and
521 suggests that the processes are somehow related.

522 More work is needed to attempt to constrain the amount of silicic acid leakage before
523 accepting that a SALH-scenario was responsible for the enhanced sedimentary opal observed
524 in ODP 1063 during MIS 4. Additional comparisons of thorium-normalised opal flux rates

525 with other proxies (for example, past eolian silica input) are required in order to better
526 understand the controls on diatom export productivity at the Bermuda Rise.

527 The most fundamental component of the SALH is its prediction of a decrease in the
528 low latitude export ratio of inorganic to organic carbon ($CaCO_3$:C_{org} rain ratio) [*Matsumoto et*
529 *al.*, 2002; *Matsumoto and Sarmiento*, 2008]. Hence, if the increase in diatom productivity
530 observed here caused a change in the $CaCO_3$:C_{org} rain ratio, it should be manifest in the
531 record of pCO_2 [*Archer et al.*, 2000; *Sigman and Boyle*, 2000]. The timing of the initiation of
532 the changes in our Nd and Si isotope records suggest that the SALH was probably not a
533 primary driver of the ~ 46 ppmv pCO_2 drawdown that occurred across the MIS 5a/4
534 transition [*Ahn and Brook*, 2008], although age model uncertainty does potentially allow for a
535 much closer association (within ~1ka) of the change in pCO_2, with the initiation of significant
536 changes in the ε_{Nd} and $\delta^{30}Si$ records in MD99-2198 (see Figure 5).

537 Nonetheless, the SALH is still likely to have provided an additional feedback that
538 contributed to the low glacial values of pCO_2. A box-modelling study of the SALH scenario
539 suggested that the potential pCO_2 drawdown associated with low-latitude changes in the
540 carbonate pump and carbon compensation feedbacks could cause a 35-45ppmv reduction in
541 pCO_2 (this could be larger if a GCM was employed) [*Matsumoto et al.*, 2002]. This finding
542 leaves open the possibility that the SALH may have had a significant impact on pCO_2
543 drawdown during MIS 4, however, our data suggest that the pCO_2 drawdown associated with
544 the SALH probably occurred over longer timescales. The rapid pCO_2 decrease seen during
545 MIS 4 is therefore a likely result of some combination of physical oceanographic
546 mechanisms, with further significant contributions from marine biota [*Hain et al.*, 2010;
547 *Sigman et al.*, 2010; *Thornalley et al.,* 2012, submitted ms].

548

549 *Conclusions*

550 Our ε_{Nd} and $\delta^{30}Si$ records from the Tobago Basin provide the first direct evidence of
551 silica leakage in glacial-aged AAIW. Patterns of opal production in the eastern equatorial
552 Atlantic, and sedimentary opal content in the northwest Atlantic during MIS 4 support the
553 interpretation of silicic acid leakage to low latitudes, and subsequent enhancement of silica-
554 based primary productivity over carbonate-based primary productivity, consistent with the
555 SALH. Based on our records, the SALH was probably not the primary driver of the 46 ppmv
556 pCO_2 decrease observed at the initiation of MIS 4, but could nonetheless have contributed to
557 pCO_2 drawdown later in MIS 4 with the development of full glacial conditions.

558

559 **Acknowledgements**

560 We thank Dirk Nürnberg (MARUM Kiel) for assistance with sampling MD99-2198; Rusty
561 Lotti and George Lozefski (Lamont-Doherty Earth Observatory Deep-Sea Sample
562 Repository) for assistance with sampling RC24-01, and Rebecca Pyne for sampling ODP
563 1063. We thank Julia Becker for running stable isotope samples, Rainer Zahn for MD99-
564 2198 benthic $\delta^{18}O$ data, Marty Fleisher for laboratory assistance and helpful discussion in
565 obtaining protactinium and thorium data on RC24-01 at Lamont-Doherty Earth Observatory;
566 and Katharina Kreissig, Claire Huck and Carys Cook (MAGIC Group Imperial College
567 London) for laboratory assistance and running of extra neodymium samples. The work is part
568 of a wider project on the MIS 5/4 transition, supervised by SB and supported by NERC (UK)
569 grant NE/F002734/1. KRH is funded by National Science Foundation grant MCG-1029986.
570 Si isotope samples were analysed at the WHOI ICP Facility. TvdF acknowledges funding
571 from the European Commission (IRG 230828).

References

Abrantes, F. (2000), 200,000 yr diatom records from Atlantic upwelling sites reveal maximum productivity during LGM and a shift in phytoplankton community structure at 185,000 yr, *Earth and Planetary Science Letters*, *176*(1), 7-16.

Abrantes, F. (2001), Assessing the *Ethmodiscus* ooze problem: new perspective from a study of an eastern equatorial Atlantic core, *Deep-Sea Research Part I-Oceanographic Research Papers*, *48*(1), 125-135.

Abrantes, F. (2003), A 340,000 year continental climate record from tropical Africa – news from opal phytoliths from the equatorial Atlantic, *Earth and Planetary Science Letters*, *209*(1–2), 165-179.

Ahn, J., and E. J. Brook (2008), Atmospheric CO_2 and Climate on Millennial Time Scales During the Last Glacial Period, *Science*, *322*(5898), 83-85.

Andersen, K. K., et al. (2007), Greenland Ice Core Chronology 2005 (GICC05) and 20 year means of oxygen isotope data from ice core NGRIP., in *Pangaea*, edited.

Anderson, R. F., and A. P. Fleer (1982), Determination of natural actinides and plutonium in marine particulate material, *Analytical Chemistry*, *54*(7), 1142-1147.

Anderson, R. F., N. Kumar, R. A. Mortlock, P. N. Froelich, P. Kubik, B. Dittrich-Hannen, and M. Suter (1998), Late-Quaternary changes in productivity of the Southern Ocean, *Journal of Marine Systems*, *17*(1-4), 497-514.

Anderson, R. F., S. Ali, L. I. Bradtmiller, S. H. H. Nielsen, M. Q. Fleisher, B. E. Anderson, and L. H. Burckle (2009), Wind-Driven Upwelling in the Southern Ocean and the Deglacial Rise in Atmospheric CO_2, *Science*, *323*(5920), 1443-1448.

Aoki, S., M. Hariyama, H. Mitsudera, H. Sasaki, and Y. Sasai (2007), Formation regions of Subantarctic Mode Water detected by OFES and Argo profiling floats, *Geophys. Res. Lett.*, *34*(10), L10606, doi: 10.1029/2007GL029828.

Archer, D., and E. Maier-Reimer (1994), Effect of deep-sea sedimentary calcite preservation on atmospheric CO_2 concentration, *Nature*, *367*(6460), 260-263.

Archer, D., A. Winguth, D. Lea, and N. Mahowald (2000a), What caused the glacial/interglacial atmospheric pCO_2 cycles?, *Rev. Geophys.*, *38*(2), 159-189, doi: 10.1029/1999RG000066.

Bacon, M. P. (1984), Glacial to interglacial changes in carbonate and clay sedimentation in the Atlantic Ocean estimated from 230Th measurements, *Chemical Geology*, *46*(2), 97-111.

Barnola, J. M., D. Raynaud, Y. S. Korotkevich, and C. Lorius (1987), Vostok ice core provides 160,000-year record of atmospheric CO_2, *Nature*, *329*(6138), 408-414.

Bayon, G., C. R. German, R. M. Boella, J. A. Milton, R. N. Taylor, and R. W. Nesbitt (2002), An improved method for extracting marine sediment fractions and its application to Sr and Nd isotopic analysis, *Chemical Geology*, *187*(3–4), 179-199.

Berger, W. H. (1982), Increase of carbon dioxide in the atmosphere during deglaciation: the coral reef hypothesis., *Naturwissenschaften*, *69*, 87-88.

Bertram, C. J., and H. Elderfield (1993), The geochemical balance of the rare earth elements and neodymium isotopes in the oceans, *Geochimica et Cosmochimica Acta*, *57*(9), 1957-1986.

Bourles, B., R. L. Molinari, E. Johns, W. D. Wilson, and K. D. Leaman (1999), Upper layer currents in the western tropical North Atlantic (1989-1991), *J. Geophys. Res.*, *104*(C1), 1361-1375, doi: 10.1029/1998jc900025.

Bowles, F. A., and P. Fleischer (1985), Orinoco and Amazon River sediment input to the eastern Caribbean Basin, *Marine Geology*, *68*(1–4), 53-72.

Bradtmiller, L. I., R. F. Anderson, M. Q. Fleisher, and L. H. Burckle (2007), Opal burial in the equatorial Atlantic Ocean over the last 30 ka: Implications for glacial-interglacial changes in the ocean silicon cycle, *Paleoceanography*, *22*(4), PA4216, doi: 10.1029/2007PA001443.

Broecker, W. S. (1982), Glacial to interglacial changes in ocean chemistry, *Progress In Oceanography*, *2*, 151-197.

Brzezinski, M. A., and D. M. Nelson (1995), The annual silica cycle in the Sargasso Sea near Bermuda, *Deep Sea Research Part I: Oceanographic Research Papers*, *42*(7), 1215-1237.

Brzezinski, M. A., D. M. Nelson, V. M. Franck, and D. E. Sigmon (2001), Silicon dynamics within an intense open-ocean diatom bloom in the Pacific sector of the Southern Ocean, *Deep Sea Research Part II: Topical Studies in Oceanography*, *48*(19-20), 3997-4018.

Brzezinski, M. A., C. J. Pride, V. M. Franck, D. M. Sigman, J. L. Sarmiento, K. Matsumoto, N. Gruber, G. H. Rau, and K. H. Coale (2002), A switch from $Si(OH)_4$ to NO_3^- depletion in the glacial Southern Ocean, *Geophys. Res. Lett.*, *29*(12), 1564-1567, doi: 10.1029/2001GL014349.

Brzezinski, M. A., et al. (2011), Co-limitation of diatoms by iron and silicic acid in the equatorial Pacific, *Deep Sea Research Part II: Topical Studies in Oceanography*, *58*(3-4), 493-511.

Bub, F. L., and W. S. Brown (1996), Intermediate layer water masses in the western tropical Atlantic Ocean, *J. Geophys. Res.*, *101*(C5), 11903-11922, doi: 10.1029/95JC03372.

Cardinal, D., L. Y. Alleman, J. de Jong, K. Ziegler, and L. André (2003), Isotopic composition of silicon measured by multicollector plasma source mass spectrometry in dry plasma mode, *Journal of Analytical Atomic Spectrometry*, *18*(3), 213-218.

Cardinal, D., L. Y. Alleman, F. Dehairs, N. Savoye, T.W. Trull, and L. André (2005), Relevance of silicon isotopes to Si-nutrient utilization and Si-source assessment in Antarctic waters. *Global Biogeochem. Cycles, 19***,** GB2007, doi: 10.1029/2004GB002364.

Chase, Z., R. F. Anderson, and M. Q. Fleisher (2001), Evidence from Authigenic Uranium for Increased Productivity of the Glacial Subantarctic Ocean, *Paleoceanography*, *16*(5), 468-478, doi: 10.1029/2000PA000542.

Chérubin, L. M., and P. L. Richardson (2007), Caribbean current variability and the influence of the Amazon and Orinoco freshwater plumes, *Deep Sea Research Part I: Oceanographic Research Papers*, *54*(9), 1451-1473.

Chester, R., and M. Hughes (1967), A chemical technique for the separation of ferro-manganese minerals, carbonate minerals and adsorbed trace elements from pelagic sediments *Chemical Geology*, *2*, 249-262.

Crosta, X., C. Beucher, K. Pahnke, and M. A. Brzezinski (2007), Silicic acid leakage from the Southern Ocean: Opposing effects of nutrient uptake and oceanic circulation, *Geophysical Research Letters*, *34*(13), doi: 10.1029/2006GL029083.

Cruz, F. W., S. J. Burns, I. Karmann, W. D. Sharp, M. Vuille, A. O. Cardoso, J. A. Ferrari, P. L. Silva Dias, and O. Viana (2005), Insolation-driven changes in atmospheric circulation over the past 116,000 years in subtropical Brazil, *Nature*, *434*(7029), 63-66.

Curry, W. B., and D. W. Oppo (2005), Glacial water mass geometry and the distribution of d13C of TCO_2 in the western Atlantic Ocean, *Paleoceanography*, *20*(1), PA1017, doi: 10.1029/2004PA001021.

de Ruijter, W. P. M., A. Biastoch, S. S. Drijfhout, J. R. E. Lutjeharms, R. P. Matano, T. Pichevin, P. J. van Leeuwen, and W. Weijer (1999), Indian-Atlantic interocean exchange: Dynamics, estimation and impact, *J. Geophys. Res.*, *104*(C9), 20885-20910. doi: 10.1029/1998JC900099.

DeMaster, D. J., W. O. Smith Jr, D. M. Nelson, and J. Y. Aller (1996), Biogeochemical processes in Amazon shelf waters: chemical distributions and uptake rates of silicon, carbon and nitrogen, *Continental Shelf Research*, *16*(5-6), 617-643.

de Souza, G. F., B. C. Reynolds, J. Rickli, M. Frank, M. A. Sato, L. J. A. Gerringa and B. Bourdon (2012), Southern Ocean control of silicon stable isotope distribution in the deep Atlantic Ocean, *Global Biogeochem. Cycles*, *26*(2), GB2035, doi: 10.1029/2011gb004141.

Egge, J. K., and D. L. Aksnes (1992), Silicate as regulating nutrient in phytoplankton competition, *Marine Ecology Progress Series*, *83*, 281-289.

Elmore, A. C., E. L. Sikes, M. S. Cook, B. Schiraldi, and T. Guilderson (2011), Enhanced Southern Ocean Ventilation Through the Last Deglaciation., paper presented at American Geophysical Union Fall Meeting San Francisco, California.

Fleisher, M. Q., and R. F. Anderson (2003), Assessing the collection efficiency of Ross Sea sediment traps using ^{230}Th and ^{231}Pa, *Deep Sea Research Part II: Topical Studies in Oceanography*, *50*(3-4), 693-712.

Flores, J. A., M. A. Bárcena, and F. J. Sierro (2000), Ocean-surface and wind dynamics in the Atlantic Ocean off Northwest Africa during the last 140 000 years, *Palaeogeography, Palaeoclimatology, Palaeoecology*, *161*(3–4), 459-478.

Foster, G.L., D. Vance and J. Prytulak (2007), No change in the neodymium isotope composition of deep water exported from the North Atlantic on glacial-interglacial time scales, *Geology, 35*(1), 37-40.

Francois, R., M. Frank, M. M. Rutgers van der Loeff, and M. P. Bacon (2004), 230Th normalization: An essential tool for interpreting sedimentary fluxes during the late Quaternary, *Paleoceanography*, *19*(1), PA1018, doi: 10.1029/2003pa000939.

Gardner, J. V., and L. H. Burckle (1975), Upper Pleistocene Ethmodiscus rex oozes from the eastern equatorial Atlantic, *Micropaleontology*, *21*(2), 236-242.

Georg, R. B., B. C. Reynolds, M. Frank, and A. N. Halliday (2006), New sample preparation techniques for the determination of Si isotopic composition using MC-ICPMS, *Chemical Geology*, *235*, 95-104.

Georg, R. B., A.J. West, A.R. Basu, and A.N. Halliday (2009), Silicon fluxes and isotope composition of direct groundwater discharge into the Bay of Bengal and the effect on the global ocean silicon isotope budget. *Earth and Planetary Science Letters, 283*, 67-74.

Gil, I. M., L. D. Keigwin, and F. G. Abrantes (2009), Deglacial diatom productivity and surface ocean properties over the Bermuda Rise, northeast Sargasso Sea, *Paleoceanography*, *24*(4), PA4101, doi: 10.1029/2008PA001729.

Goldstein, S. L., R. K. O'Nions, and P. J. Hamilton (1984), A Sm-Nd isotopic study of atmospheric dusts and particulates from major river systems, *Earth and Planetary Science Letters*, *70*(2), 221-236.

Goldstein, S. L., N. T. Arndt, and R. F. Stallard (1997), The history of a continent from U□Pb ages of zircons from Orinoco River sand and Sm□Nd isotopes in Orinoco basin river sediments, *Chemical Geology*, *139*(1–4), 271-286.

Group, T. R. (1981), Gulf Stream Cold-Core Rings: Their Physics, Chemistry, and Biology, *Science*, *212*(4499), 1091-1100.

Grützner, J., et al. (2002), Astronomical age models for Pleistocene drift sediments from the western North Atlantic (ODP Sites 1055–1063), *Marine Geology*, *189*(1–2), 5-23.

Guihou, A., S. Pichat, S. Nave, A. Govin, L. Labeyrie, E. Michel, and C. Waelbroeck (2010), Late slowdown of the Atlantic Meridional Overturning Circulation during the Last Glacial Inception: New constraints from sedimentary (231Pa/230Th), *Earth and Planetary Science Letters*, *289*(3-4), 520-529.

Gutjahr, M., M. Frank, C. H. Stirling, L. D. Keigwin, and A. N. Halliday (2008), Tracing the Nd isotope evolution of North Atlantic Deep and Intermediate Waters in the western North Atlantic since the Last Glacial Maximum from Blake Ridge sediments, *Earth and Planetary Science Letters*, *266*(1–2), 61-77.

Gutjahr, M., M. Frank, C. H. Stirling, V. Klemm, T. van de Flierdt, and A. N. Halliday (2007), Reliable extraction of a deepwater trace metal isotope signal from Fe-Mn oxyhydroxide coatings of marine sediments, *Chemical Geology*, *242*(3-4), 351-370.

Haddad, G. A., and A. W. Droxler (1996), Metastable CaCO3 Dissolution at Intermediate Water Depths of the Caribbean and Western North Atlantic: Implications for Intermediate Water Circulation During the Past 200,000 Years, *Paleoceanography*, *11*(6), 701-716, doi: 10.1029/96PA02406.

Hain, M. P., D. M. Sigman, and G. H. Haug (2010), Carbon dioxide effects of Antarctic stratification, North Atlantic Intermediate Water formation, and subantarctic nutrient drawdown during the last ice age: Diagnosis and synthesis in a geochemical box model, *Global Biogeochem. Cycles*, *24*(4), GB4023, doi 10.1029/2010GB003790.

Haley, B. A., G. P. Klinkhammer, and J. McManus (2004), Rare earth elements in pore waters of marine sediments, *Geochimica et Cosmochimica Acta*, *68*(6), 1265-1279.
Hanawa, K., and L. D. Talley (2001), Mode Waters, in *Ocean Circulation and Climate*, edited by G. Siedler and J. Church, pp. 373-386, Academic Press, International Geophysics Series, San Diego.
Heath, G. R. (1974), Dissolved silica and deep-sea sediments, in *Soc. Econ. Paleont. Mineral. Spec. Publ.*, edited by W. W. Hay, pp. 77-93.
Hendry, K. R., R. B. Georg, R. E. M. Rickaby, L. F. Robinson, and A. N. Halliday (2010), Deep ocean nutrients during the Last Glacial Maximum deduced from sponge silicon isotopic compositions, *EPSL*, *292*, 290-300.
Hendry, K. R., M. J. Leng, L. F. Robinson, H. J. Sloane, J. Blusztjan, R. E. M. Rickaby, R. B. Georg and A. N. Halliday (2011), Silicon isotopes in Antarctic sponges: an interlaboratory comparison, *Antarctic Science, 23*(1), 34-42.
Hendry, K. R., and L. F. Robinson (2012), The relationship between silicon isotope fractionation in sponges and silicic acid concentration: modern and core-top studies of biogenic opal, *Geochimica et Cosmochimica Acta*, *81*, 1-12.
Herwitz, S. R., D. R. Muhs, J. M. Prospero, S. Mahan, and B. Vaughn (1996), Origin of Bermuda's clay-rich Quaternary paleosols and their paleoclimatic significance, *J. Geophys. Res.*, *101*(D18), 23389-23400, doi: 10.1029/96JD02333.
Hodell, D. A., K. A. Venz, C. D. Charles, and U. S. Ninnemann (2003), Pleistocene vertical carbon isotope and carbonate gradients in the South Atlantic sector of the Southern Ocean, *Geochem. Geophys. Geosyst.*, *4*(1), 1004, doi: 10.1029/2002GC000367.
Höll, C., B. Karwath, C. Rühlemann, K. A. F. Zonneveld, and H. Willems (1999), Palaeoenvironmental information gained from calcareous dinoflagellates: the late Quaternary eastern and western tropical Atlantic Ocean in comparison, *Palaeogeography, Palaeoclimatology, Palaeoecology*, *146*(1–4), 147-164.
Hüls, M., and R. Zahn (2000), Millennial-Scale Sea Surface Temperature Variability in the Western Tropical North Atlantic from Planktonic Foraminiferal Census Counts, *Paleoceanography*, *15*(6), 659-678, doi: 10.1029/1999PA000462.
Jacobsen, S. B., and G. J. Wasserburg (1980), Sm-Nd isotopic evolution of chondrites, *Earth and Planetary Science Letters*, *50*(1), 139-155.
Jansen, J. H. F., E. Ufkes, and R. R. Schneider (1996), Late Quaternary movements of the Angola-Benguela Front SE Atlantic and implications for advection in the equatorial ocean., in *The South Atlantic: Past and Present Circulation*, edited by G. Wefer, W. H. Berger, G. Siedler and D. J. Webb, pp. 553-575, Springer-Verlag, Berlin.
Jeandel, C. (1993), Concentration and isotopic composition of Nd in the South Atlantic Ocean, *Earth and Planetary Science Letters*, *117*(3-4), 581-591.
Jeandel, C., D. Thouron, and M. Fieux (1998), Concentrations and isotopic compositions of neodymium in the eastern Indian Ocean and Indonesian straits, *Geochimica et Cosmochimica Acta*, *62*(15), 2597-2607.
Keigwin, L. D., W. B. Curry, S. J. Lehman and S. Johnsen (1994), The role of the deep ocean in North Atlantic climate change between 70 and 130 kyr ago, *Nature*, *371*(6495), 323-326.
Keigwin, L. D., and E. A. Boyle (2008), Did North Atlantic overturning halt 17,000 years ago?, *Paleoceanography*, *23*(1), PA1101, doi: 10.1029/2007PA001500.
Krause, J. W., M. W. Lomas, and D. M. Nelson (2009), Biogenic silica at the Bermuda Atlantic Time-series Study site in the Sargasso Sea: Temporal changes and their inferred controls based on a 15-year record, *Global Biogeochem. Cycles*, *23*(3), GB3004, doi: 10.1029/2008GB003236.
Kumar, N., R. F. Anderson, R. A. Mortlock, P. N. Froelich, P. Kubik, B. Dittrich-Hannen, and M. Suter (1995), Increased biological productivity and export production in the glacial Southern Ocean, *Nature*, *378*(6558), 675-680.
Lacan, F., and C. Jeandel (2005), Acquisition of the neodymium isotopic composition of the North Atlantic Deep Water, *Geochem. Geophys. Geosyst.*, *6*(12), Q12008, doi: 10.1029/2005GC000956.

Laine, E. P., and C. D. Hollister (1981), Geological effects of the Gulf Stream System on the northern Bermuda Rise, *Marine Geology*, *39*(3-4), 277-310.
Lea, D. W., D. K. Pak, L. C. Peterson, and K. A. Hughen (2003), Synchroneity of Tropical and High-Latitude Atlantic Temperatures over the Last Glacial Termination, *Science*, *301*(5638), 1361-1364.
Levitus, S., M. E. Conkright, J. L. Reid, R. G. Najjar, and A. Mantyla (1993), Distribution of nitrate, phosphate and silicate in the world oceans, *Progress In Oceanography*, *31*(3), 245-273.
Lewis, W., and J. Saunders (1989), Concentration and transport of dissolved and suspended substances in the Orinoco River, *Biogeochemistry*, *7*(3), 203-240.
Lippold, J., J. Grützner, D. Winter, Y. Lahaye, A. Mangini, and M. Christl (2009), Does sedimentary 231Pa/230Th from the Bermuda Rise monitor past Atlantic Meridional Overturning Circulation?, *Geophys. Res. Lett.*, *36*(12), L12601, 10.1029/2009GL038068.
Marchitto, T. M., and W. S. Broecker (2006), Deep water mass geometry in the glacial Atlantic Ocean: A review of constraints from the paleonutrient proxy Cd/Ca, *Geochem. Geophys. Geosyst.*, *7*(12), Q12003, 10.1029/2006GC001323.
Martin, J. H. (1990), Glacial-Interglacial CO_2 Change: The Iron Hypothesis, *Paleoceanography*, *5*(1), 1-13, doi: 10.1029/PA005i001p00001.
Martínez-Méndez, G., R. Zahn, I. R. Hall, F. J. C. Peeters, L. D. Pena, I. Cacho, and C. Negre (2010), Contrasting multiproxy reconstructions of surface ocean hydrography in the Agulhas Corridor and implications for the Agulhas Leakage during the last 345,000 years, *Paleoceanography*, *25*(4), PA4227, doi: 10.1029/2009PA001879.
Matsumoto, K., and J. L. Sarmiento (2008), A corollary to the silicic acid leakage hypothesis, *Paleoceanography*, *23*(2), PA2203, doi: 10.1029/2007PA001515.
Matsumoto, K., J. L. Sarmiento, and M. A. Brzezinski (2002), Silicic acid leakage from the Southern Ocean: A possible explanation for glacial atmospheric pCO_2, *Global Biogeochem. Cycles*, *16*(3), 1031, doi: 10.1029/2001GB001442.
McCartney, M. S. (1977), Subantarctic Mode Water, in *A Voyage of Discovery*, edited by M. Angel, pp. 103-119, Pergamon.
McManus, J. F., R. Francois, J. M. Gherardi, L. D. Keigwin, and S. Brown-Leger (2004), Collapse and rapid resumption of Atlantic meridional circulation linked to deglacial climate changes, *Nature*, *428*(6985), 834-837.
Meredith, M. P., K. E. Grose, E. L. McDonagh, K. J. Heywood, R. D. Frew, and P. F. Dennis (1999), Distribution of oxygen isotopes in the water masses of Drake Passage and the South Atlantic, *J. Geophys. Res.*, *104*(C9), 20949-20962, doi: 10.1029/98jc02544.
Molleri, G. S. F., E. M. L. d. M. Novo, and M. Kampel (2010), Space-time variability of the Amazon River plume based on satellite ocean color, *Continental Shelf Research*, *30*(3–4), 342-352.
Mortlock, R. A., and P. N. Froelich (1989), A simple method for the rapid determination of biogenic opal in pelagic marine sediments, *Deep Sea Research Part A. Oceanographic Research Papers*, *36*(9), 1415-1426.
Nelson, D. M., and M. A. Brzezinski (1997), Diatom growth and productivity in an oligotrophic midocean gyre: A 3-yr record from the Sargasso Sea near Bermuda, *Limnology & Oceanography*, *43*, 473-486.
Nelson, D. M., P. Tréguer, M. A. Brzezinski, A. Leynaert, and B. Quéguiner (1995), Production and dissolution of biogenic silica in the ocean: Revised global estimates, comparison with regional data and relationship to biogenic sedimentation, *Global Biogeochem. Cycles*, *9*(3), 359-372, doi: 10.1029/95gb01070.
Pahnke, K., and R. Zahn (2005), Southern Hemisphere Water Mass Conversion Linked with North Atlantic Climate Variability, *Science*, *307*(5716), 1741-1746.
Pahnke, K., S. L. Goldstein, and S. R. Hemming (2008), Abrupt changes in Antarctic Intermediate Water circulation over the past 25,000 years, *Nature Geoscience*, *1*, 870-874.

Peeters, F. J. C., R. Acheson, G.-J. A. Brummer, W. P. M. de Ruijter, R. R. Schneider, G. M. Ganssen, E. Ufkes, and D. Kroon (2004), Vigorous exchange between the Indian and Atlantic oceans at the end of the past five glacial periods, *Nature*, *430*(7000), 661-665.

Peterson, L. C., and G. H. Haug (2006), Variability in the mean latitude of the Atlantic Intertropical Convergence Zone as recorded by riverine input of sediments to the Cariaco Basin (Venezuela), *Palaeogeography, Palaeoclimatology, Palaeoecology*, *234*(1), 97-113.

Peterson, L. C., G. H. Haug, K. A. Hughen, and U. Röhl (2000), Rapid Changes in the Hydrologic Cycle of the Tropical Atlantic During the Last Glacial, *Science*, *290*(5498), 1947-1951.

Petit, J. R., et al. (1999), Climate and atmospheric history of the past 420,000 years from the Vostok ice core, Antarctica, *Nature*, *399*(6735), 429-436.

Piepgras, D. J., and G. J. Wasserburg (1980), Neodymium isotopic variations in seawater, *Earth and Planetary Science Letters*, *50*(1), 128-138.

Piepgras, D. J., and G. J. Wasserburg (1982), Isotopic Composition of Neodymium in Waters from the Drake Passage, *Science*, *217*(4556), 207-214.

Piepgras, D. J., and G. J. Wasserburg (1987), Rare earth element transport in the western North Atlantic inferred from Nd isotopic observations, *Geochimica et Cosmochimica Acta*, *51*(5), 1257-1271.

Piola, A. R., and D. T. Georgi (1982), Circumpolar properties of Antarctic intermediate water and Subantarctic Mode Water, *Deep Sea Research Part A. Oceanographic Research Papers*, *29*(6), 687-711.

Piotrowski, A. M., S. L. Goldstein, S. R. Hemming, and R. G. Fairbanks (2005), Temporal Relationships of Carbon Cycling and Ocean Circulation at Glacial Boundaries, *Science*, *307*(5717), 1933-1938.

Piotrowski, A. M., S. L. Goldstein, H. S. R, R. G. Fairbanks, and D. R. Zylberberg (2008), Oscillating glacial northern and southern deep water formation from combined neodymium and carbon isotopes, *Earth and Planetary Science Letters*, *272*(1-2), 394-405.

Pondaven, P., O. Ragueneau, P. Treguer, A. Hauvespre, L. Dezileau, and J. L. Reyss (2000), Resolving the `opal paradox' in the Southern Ocean, *Nature*, *405*(6783), 168-172.

Ragueneau, O., et al. (2000), A review of the Si cycle in the modern ocean: recent progress and missing gaps in the application of biogenic opal as a paleoproductivity proxy, *Global and Planetary Change*, *26*(4), 317-365.

Robinson, L. F., and T. van de Flierdt (2009), Southern Ocean evidence for reduced export of North Atlantic Deep Water during Heinrich event 1, *Geology*, *37*(3), 195-198.

Rogerson, M., P. P. E. Weaver, E. J. Rohling, L. J. Lourens, J. W. Murray, and A. Hayes (2006), Colour logging as a tool in high-resolution palaeoceanography, in *New Techniques in Sediment Core Analysis*, edited by R. G. Rothwell, pp. 99-112, Geological Society (Special Publications), London.

Rühlemann, C., M. Frank, W. Hale, A. Mangini, S. Mulitza, P. J. Müller, and G. Wefer (1996), Late Quaternary productivity changes in the western equatorial Atlantic: Evidence from 230Th-normalized carbonate and organic carbon accumulation rates, *Marine Geology*, *135*(1–4), 127-152.

Rutberg, R. L., S. R. Hemming, and S. L. Goldstein (2000), Reduced North Atlantic Deep Water flux to the glacial Southern Ocean inferred from neodymium isotope ratios, *Nature*, *405*(6789), 935-938.

Sarmiento, J. L., and J. R. Toggweiler (1984), A new model for the role of the oceans in determining atmospheric pCO_2, *Nature*, *308*(5960), 621-624.

Sarmiento, J. L., N. Gruber, M. A. Brzezinski, and J. P. Dunne (2004), High-latitude controls of thermocline nutrients and low latitude biological productivity, *Nature*, *427*(6969), 56-60.

Sarnthein, M., U. Pflaumann, R. Ross, R. Tiedemann, and K. Winn (1992), Transfer functions to reconstruct ocean palaeoproductivity: a comparison, in *Upwelling Systems: Evolution Since the Early Miocene*, edited by C. P. Summerhayes, W. L. Prell and K. C. Emeis, pp. 411-427, Geological Society Special Publication.

Schlitzer, R. (2000), Electronic Atlas of WOCE Hydrographic and Tracer data now available, *Eos Trans AGU*, *81*.

870 Sievers, H. A., and W. D. Nowlin, Jr. (1984), The Stratification and Water Masses at Drake Passage, *J.*
871 *Geophys. Res.*, *89*(C6), 10489-10514, doi: 10.1029/JC089iC06p10489.
872 Sigman, D. M., and E. A. Boyle (2000), Glacial/interglacial variations in atmospheric carbon dioxide,
873 *Nature*, *407*(6806), 859-869.
874 Sigman, D. M., M. P. Hain, and G. H. Haug (2010), The polar ocean and glacial cycles in atmospheric
875 CO_2 concentration, *Nature*, *466*(7302), 47-55.
876 Stabell, B. (1986), Variations of Diatom Flux in the Eastern Equatorial Atlantic During the Last
877 400,000 Years (METEOR Cores 13519 and 13521), *Marine Geology*, *72*(3-4), 305-323.
878 Stichel, T., M. Frank, J. Rickli and B. A. Haley (2012), The hafnium and neodymium isotope
879 composition of seawater in the Atlantic sector of the Southern Ocean, *Earth and Planetary Science*
880 *Letters, 317-318*(1), 282-294.
881 Stordal, M. C., and G. J. Wasserburg (1986), Neodymium isotopic study of Baffin Bay water: sources
882 of REE from very old terranes, *Earth and Planetary Science Letters*, *77*(3-4), 259-272.
883 Stramma, L., and F. Schott (1999), The mean flow field of the tropical Atlantic Ocean, *Deep Sea*
884 *Research Part II: Topical Studies in Oceanography*, *46*(1–2), 279-303.
885 Suga, T., and L. D. Talley (1995), Antarctic Intermediate Water circulation in the tropical and
886 subtropical South Atlantic, *Journal of Geophysical Research*, *100*(C7), 13441-13453.
887 Tachikawa, K., M. Roy-Barman, A. Michard, D. Thouron, D. Yeghicheyan and C. Jeandel (2004),
888 Neodymium isotopes in the Mediterranean Sea: comparison between seawater and sediment
889 signals, *Geochimica et Cosmochimica Acta, 68*(14), 3095-3106.
890 Takeda, S. (1998), Influence of iron availability on nutrient consumption ratio of diatoms in oceanic
891 waters, *Nature*, *393*(6687), 774-777.
892 Tanaka, T., et al. (2000), JNdi-1: a neodymium isotopic reference in consistency with LaJolla
893 neodymium, *Chemical Geology*, *168*(3–4), 279-281.
894 Thornalley, D.J.R., S. Barker, T. van de Flierdt, J. Becker, I.R. Hall and G. Knorr (2012), Abrupt changes
895 in deep Atlantic circulation during the transition to full glacial conditions, *Nature*, submitted ms.
896 Timmermans, K. R., B. Van der Wagt, and H. J. W. De Baar (2004), Growth Rates, Half-Saturation
897 Constants, and Silicate, Nitrate, and Phosphate Depletion in Relation to Iron Availability of Four
898 Large, Open-Ocean Diatoms from the Southern Ocean, *Limnology & Oceanography*, *49*(6), 2141-
899 2151.
900 Toggweiler, J. R., J. L. Russell, and S. R. Carson (2006), Midlatitude westerlies, atmospheric CO_2, and
901 climate change during the ice ages, *Paleoceanography*, *21*(2), PA2005, 10.1029/2005PA001154 .
902 Tréguer, P., D. M. Nelson, A. J. Van Bennekom, D. J. DeMaster, A. Leynaert, and B. Quéguiner (1995),
903 The silica balance in the world ocean: a reestimate, *Science*, *268*(5209), 375-379.
904 Tsuchiya, M. (1989), Circulation of the Antarctic Intermediate Water in the North Atlantic Ocean,
905 *Journal of Marine Research*, *47*(4), 747-755.
906 van de Flierdt, T., L. F. Robinson, J. F. Adkins, S. R. Hemming, and S. L. Goldstein (2006), Temporal
907 stability of the neodymium isotope signature of the Holocene to glacial North Atlantic,
908 *Paleoceanography*, *21*(4), PA4102, doi: 10.1029/2006PA001294.
909 Voelker, A. H. L., S. M. Lebreiro, J. Schönfeld, I. Cacho, H. Erlenkeuser, and F. Abrantes (2006),
910 Mediterranean outflow strengthening during northern hemisphere coolings: A salt source for the
911 glacial Atlantic?, *Earth and Planetary Science Letters*, *245*(1–2), 39-55.
912 Vuille, M., R. S. Bradley, M. Werner, R. Healy, and F. Keimig (2003), Modeling d18O in precipitation
913 over the tropical Americas: 1. Interannual variability and climatic controls, *J. Geophys. Res.*, *108*(D6),
914 4174, doi: 10.1029/2001JD002038.
915 Wang, Y., H. Cheng, R. L. Edwards, X. Kong, X. Shao, S. Chen, J. Wu, X. Jiang, X. Wang, and Z. An
916 (2008), Millennial- and orbital-scale changes in the East Asian monsoon over the past 224,000 years,
917 *Nature*, *451*(7182), 1090-1093.
918 Wang, Y. J., H. Cheng, R. L. Edwards, Z. S. An, J. Y. Wu, C.-C. Shen, and J. A. Dorale (2001), A High-
919 Resolution Absolute-Dated Late Pleistocene Monsoon Record from Hulu Cave, China, *Science*,
920 *294*(5550), 2345-2348.

Wilson, W. D., E. Johns, and R. L. Molinari (1994), Upper layer circulation in the western tropical North Atlantic Ocean during August 1989, *J. Geophys. Res.*, *99*(C11), 22513-22523, doi: 10.1029/94JC02066.
Wong, A. P. S., N. L. Bindoff, and J. A. Church (1999), Large-scale freshening of intermediate waters in the Pacific and Indian oceans, *Nature*, *400*(6743), 440-443.
Wüst, G. (1964), *Stratification and Circulation of the Antillean–Caribbean Basins: Part 1. Spreading and Mixing of the Water Types with an Oceanographic Atlas.*, Columbia University Press, New York.
Zuo, H., A. C. Naveira Garabato, A. L. New and A. Oschlies (2012), Mechanisms of subantarctic mode water upwelling in a hybrid-coordinate global GCM, *Ocean Modelling*, *45-46*(0), 59-80.

Figure captions

Figure 1- Concentrations of nitrate (top panel), silicate (middle panel) and the pseudo-tracer Si* (bottom panel) from a transect through the western Atlantic from ~75°S to 40°N, with all core locations plotted by latitude and depth (note: the hydrographic section is only relevant for MD99-2198, shown with a black marker; ODP 1063 and RC24-01 are shown by grey markers). AAIW is identifiable as a tongue of high-nitrate, low Si* water extended from high southern latitude to low latitude [*Schlitzer*, 2000]. Si* = $[Si(OH)_4] - [NO_3^-]$ [*Sarmiento et al.*, 2004]. Salinity is indicated by the contours in black (values in PSS-78) [*Schlitzer*, 2000].

Figure 2 - Core location map with marked positions of all cores used in this investigation.

Figure 3 - (a) NGRIP $\delta^{18}O$ (grey curve) [*Andersen et al.*, 2007], adjusted to the Hulu-Sanbao speleothem record [*Wang et al.*, 2001; *Wang et al.*, 2008]; (b) MD99-2198 planktic foraminiferal $\delta^{18}O$ record of *Globigerinoides ruber* (white), tuned to the NGRIP record (green curve); (c) MD99-2198 L* core reflectance [*Hüls and Zahn*, 2000] (red curve); (d) MD99-2198 core sedimentation rate (cm/ka) (black curve). Northern hemisphere cold periods are marked by grey bands.

949

950 **Figure 4 -** (a) NGRIP $\delta^{18}O$ (grey curve) [*Andersen et al.*, 2007], adjusted to the Hulu-Sanbao
951 speleothem record [*Wang et al.*, 2001; *Wang et al.*, 2008]; (b) ODP 1063 % $CaCO_3$ (red
952 curve) [*Thornalley et al.,* 2012]; (c) RC24-01 % $CaCO_3$, tuned to the NGRIP record (blue
953 curve); (d) RC24-01 sedimentation rate (cm/ka) (black curve); (e) ODP 1063 planktic
954 foraminiferal $\delta^{18}O$ (*Globorotalia inflata*) tuned to NGRIP $\delta^{18}O$ (green curve) [*Thornalley et*
955 *al.,* 2012]. Northern hemisphere cold periods are marked by grey bands.

956

957 **Figure 5 -** (a) NGRIP $\delta^{18}O$ [*Andersen et al.*, 2007], adjusted to the Hulu-Sanbao speleothem
958 record [*Wang et al.*, 2001; *Wang et al.*, 2008]; (b) MD99-2198 planktic $\delta^{18}O$ (‰); (c) MD99-
959 2198 sedimentary ε_{Nd}, error bars are 2σSD; (d) MD99-2198 sponge spicule $\delta^{30}Si$, error bars
960 are 2σSD; (e) Byrd (Antarctica) ice core pCO_2 [*Ahn and Brook*, 2008]; (f) MD99-2198 opal
961 (%, purple curve); (g) ODP 1063 opal (%, purple curve); (h) RC24-01 opal (%, purple curve);
962 (i) RC24-01 thorium-normalised preserved opal flux rate ($g/cm^2/ka$, brown curve). All
963 percent opal measurements are plotted on the same scale. Northern hemisphere cold periods
964 are marked by grey bands, and MIS 4 (orange shading), and cold D/O 19 and 20 are
965 annotated.

966

967 **Figure 6 -** A plot of the range of expected silicic acid concentrations (orange shaded area),
968 given the predicted $\delta^{30}Si$ variability of +1.5 – +2 ‰ in AAIW [*Hendry et al.*, 2010; *de Souza*
969 *et al*., 2012]. Calculated values of paleo-$[Si(OH)_4]$ assuming a $\delta^{30}Si$ for AAIW of 1.5 ‰ [*de*
970 *Souza et al.*, 2012], are shown in black.

971

Figure 7 – (a) NGRIP $\delta^{18}O$ (‰) (grey curve) [*Andersen et al.*, 2007], adjusted to the Hulu-Sanbao speleothem record [*Wang et al.*, 2001; *Wang et al.*, 2008]; (b) RC24-01 opal flux rate ($g/cm^2/ka$) (blue curve); (c) RC24-01 total organic carbon flux rate ($g/cm^2/ka$) (green curve); (d) RC24-01 authigenic uranium (dpm/g) (pink curve), used as a proxy for organic carbon flux; (e) RC24-01 total nitrogen flux rate ($g/cm^2/ka$) (brown curve). All proxies record an opal-driven increase in primary productivity in the EEA during MIS 4. Northern hemisphere cold periods are marked by grey bands, and MIS 4 (orange shading), and cold D/O 19 and 20 are annotated.

993 **Tables**

994 **Table 1 -** MD99-2198 Nd isotope data

Depth (cm)	Age (ka)	$^{143}Nd/^{144}Nd$	2 σ S.E.	ε_{Nd}	2 σ S.D.
850-851	44.62	0.512116	0.000010	-10.2	0.2
950-951	55.09	0.512159	0.000012	-9.3	0.2
1016-1017	61.79	0.512121	0.000006	-10.1	0.3
1026-1027	62.88	0.512124	0.000010	-10.0	0.3
1036-1037	63.97	0.512174	0.000014	-9.1	0.3
1046-1047	65.06	0.512130	0.000010	-9.9	0.3
1056-1057	66.15	0.512155	0.000008	-9.4	0.3
1076-1077	68.33	0.512127	0.000012	-10.0	0.3
1086-1087	69.42	0.512072	0.000012	-11.0	0.3
1106-1107	71.60	0.512087	0.000020	-10.8	0.3
1131-1132	73.01	0.512097	0.000018	-10.6	0.3
1276-1277	80.68	0.512088	0.000012	-10.7	0.3
1421-1422 *	90.50	0.512103	0.000014	-10.4	0.6

995

996

997 All reported $^{143}Nd/^{144}Nd$ ratios have been normalised to the recommended JNdi value
998 of Tanaka et al. (2000). Epsilon Nd values denote the deviation of measured $^{143}Nd/^{144}Nd$
999 values from the bulk Earth value (CHUR=0.512638) in parts per 10,000. The external
1000 reproducibility (2σSD) is reported based on repeat JNd_i analyses of the day. For one sample
1001 (*), the ion beam was significantly smaller than for standards and hence a propagated error is
1002 reported to reflect this difference.

1003 **Table 2 -** MD99-2918 Si isotope data. External reproducibility for $\delta^{30}Si$ values is +/- 0.23

1004 per mil.

Depth (cm)	Age (ka)	Mean $\delta^{30}Si$ (all analyses)	~$[Si(OH)_4]$ (µM)
850-851	44.62	-0.86	11.6
950-951	55.09	-1.13	16.0
1016-1017	61.79	-0.74	9.8
1026-1027	62.88	-0.73	9.6
1036-1037	63.97	-0.96	13.1
1046-1047	65.06	-0.43	5.5
1056-1057	66.15	-0.39	5.0
1066-1067	67.24	-0.35	4.6
1076-1077	68.33	-0.23	3.1
1086-1087	69.42	-0.12	1.9
1106-1107	71.60	-0.12	1.8
1131-1132	73.01	-0.57	7.4
1176-1177	75.55	-0.58	7.5
1276-1277	80.68	0.28	-2.2
1421-1422	90.50	0.15	-1.0

1005

1006

1007

1008

1009 **Table 3** - RC24-01 radionuclide data

Depth (cm)	Age (ka)	% opal	^{230}Th-norm F(g/cm^2/ka)	error +/-	U_{auth} (dpm/g)	error +/-
284.5	43.451	6.65	1.259	0.023	0.880	0.012
293.5	52.401	8.40	1.220	0.029	1.257	0.017
302.5	59.988	7.78	1.270	0.035	1.781	0.026
310.5	63.079	10.59	1.062	0.038	2.644	0.034
318.5	66.170	10.38	1.205	0.040	2.818	0.039
325.5	68.875	8.94	1.239	0.047	2.046	0.027
333.5	71.836	7.09	1.321	0.050	1.486	0.020
344.5	74.669	4.62	1.332	0.053	1.298	0.018
351.5	77.161	5.32	1.299	0.045	1.097	0.017
353.5	78.090	4.95	1.331	0.037	0.778	0.013
365.5	83.666	3.67	1.403	0.043	0.304	0.005
373.5	87.944	3.73	1.538	0.041	0.133	0.002

1010

1011 **Copyrighted material**

1012 This manuscript contains no material which is subject to copyright.

1013

1014

1015

1016

1017 **Figures**

1018 Figure 1

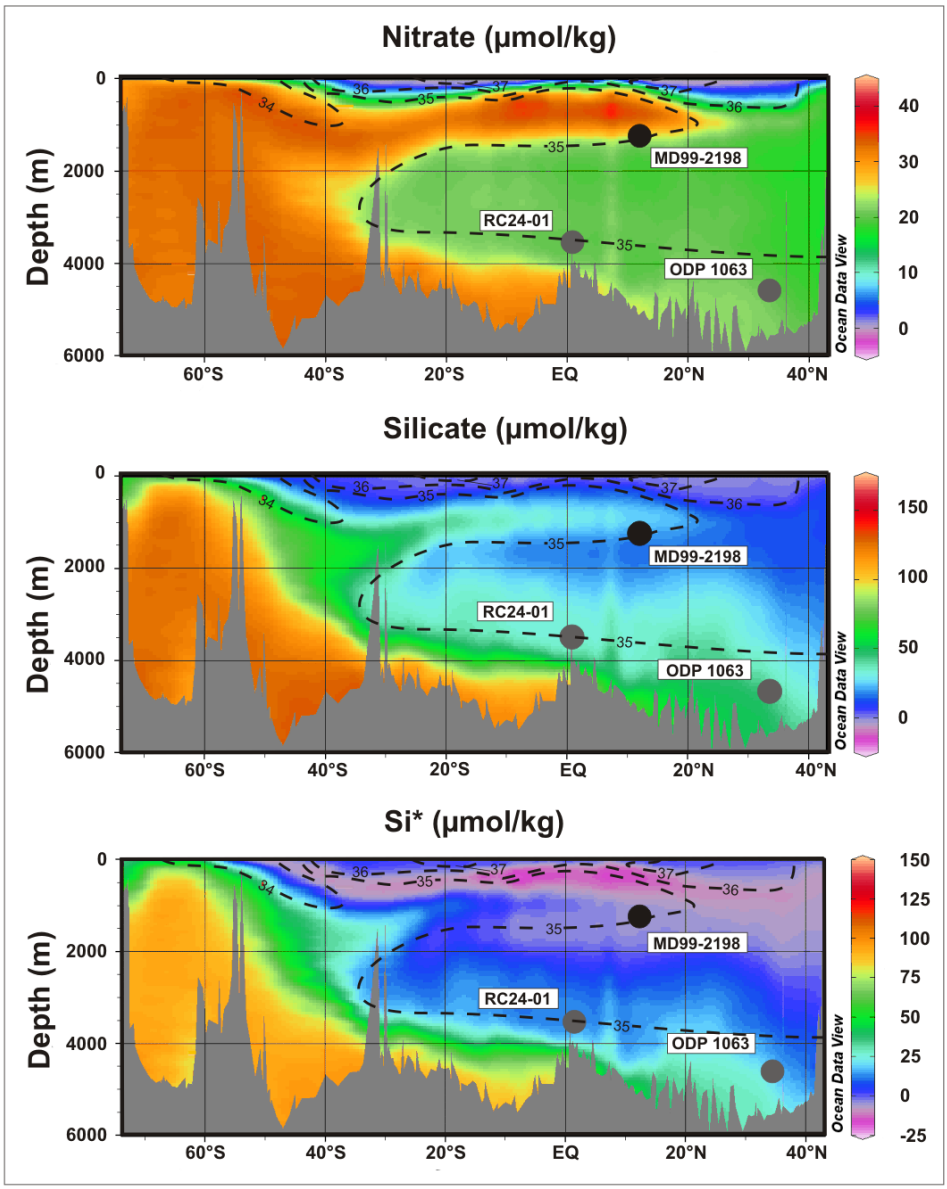

1019

1020

1021

1022

1023

Figure 2

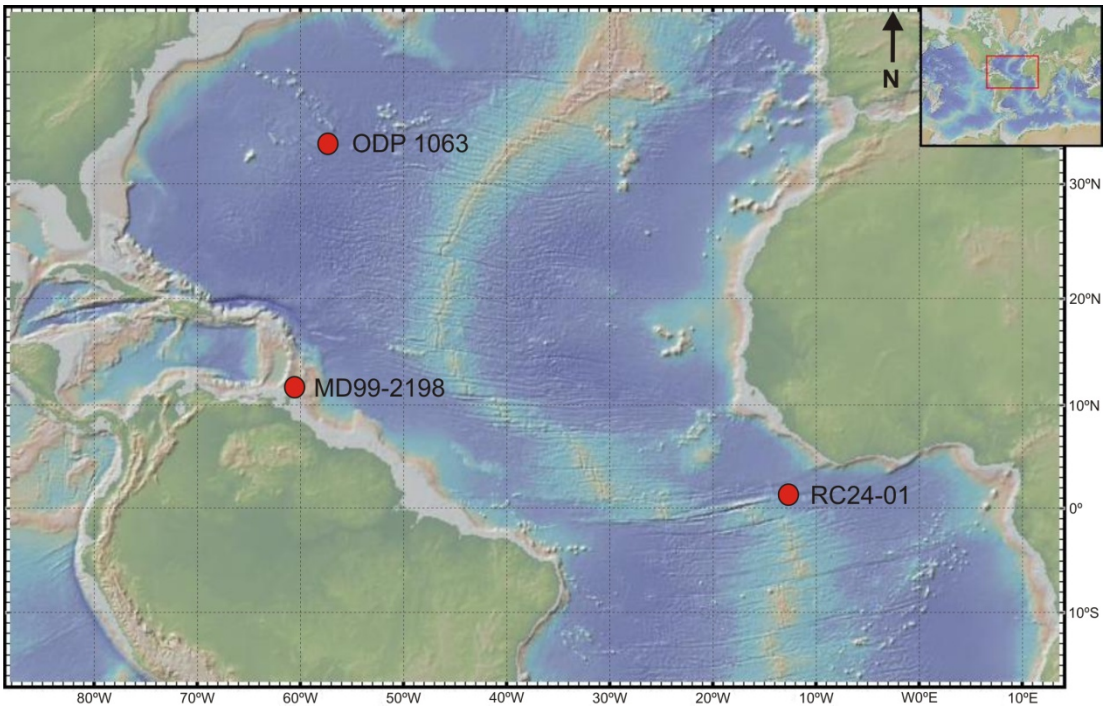
N
ODP 1063
MD99-2198
RC24-01
30°N
20°N
10°N
0°
10°S
80°W
70°W
60°W
50°W
40°W
30°W
20°W
10°W
W0°E
10°E

Figure 3

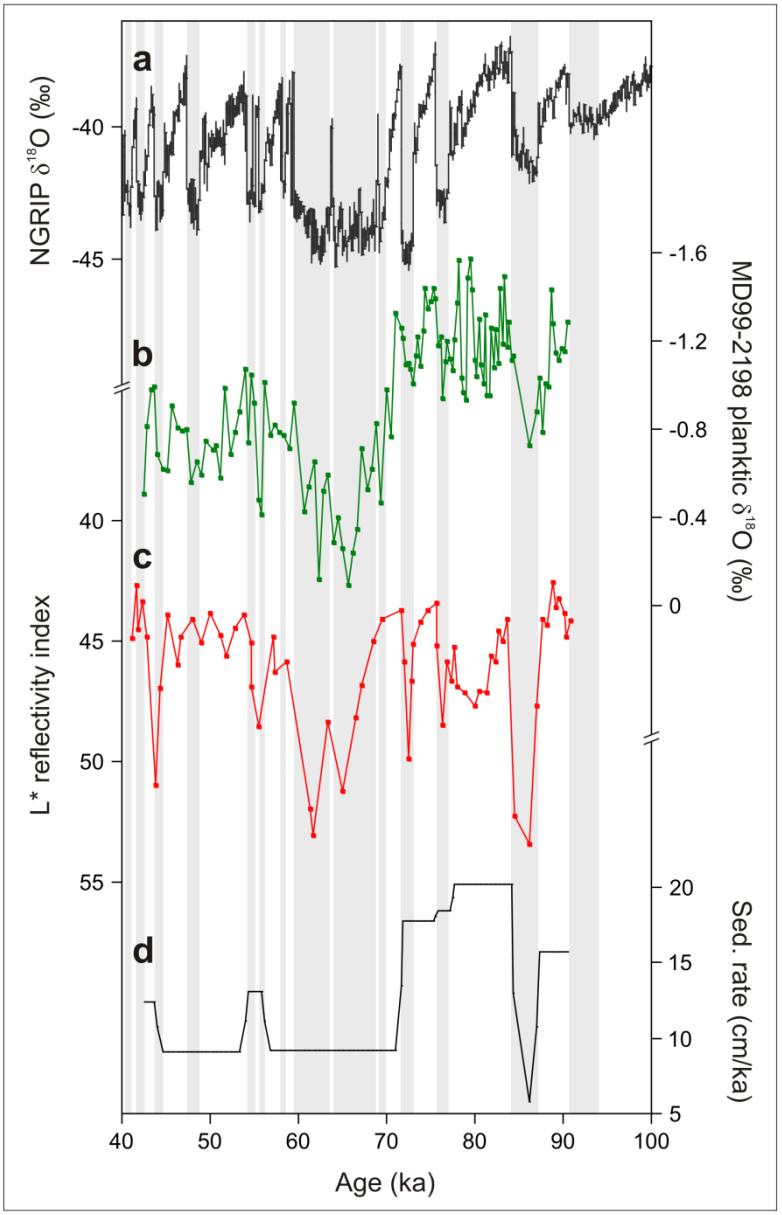
a
b
c
d
NGRIP δ18O (‰)
-40
-45
MD99-2198 planktic δ18O (‰)
-1.6
-1.2
-0.8
-0.4
0
L* reflectivity index
40
45
50
55
Sed. rate (cm/ka)
20
15
10
5
40
50
60
70
80
90
100
Age (ka)

1043 Figure 4

1044

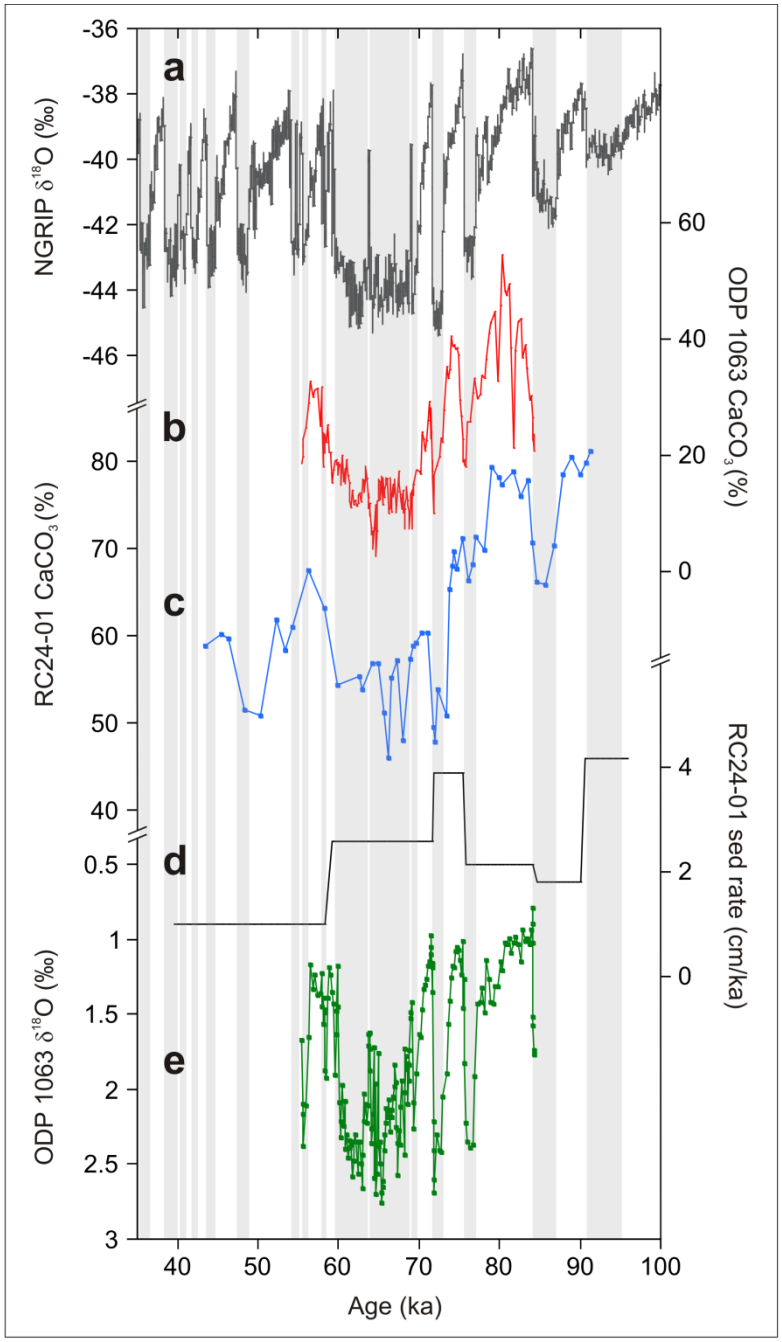

1045

1046

1047

1048

1049

Figure 5

1050

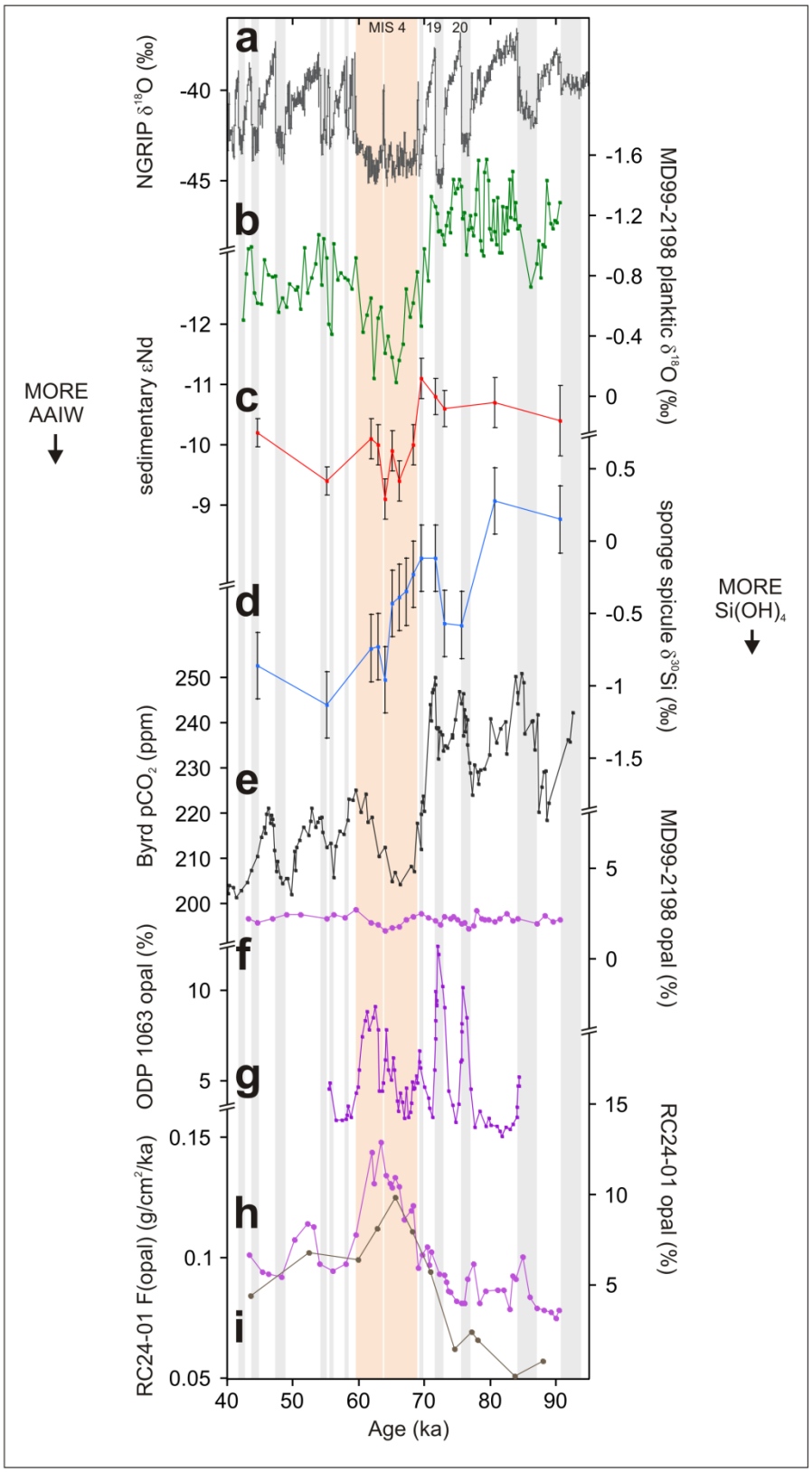

1051

Figure 6

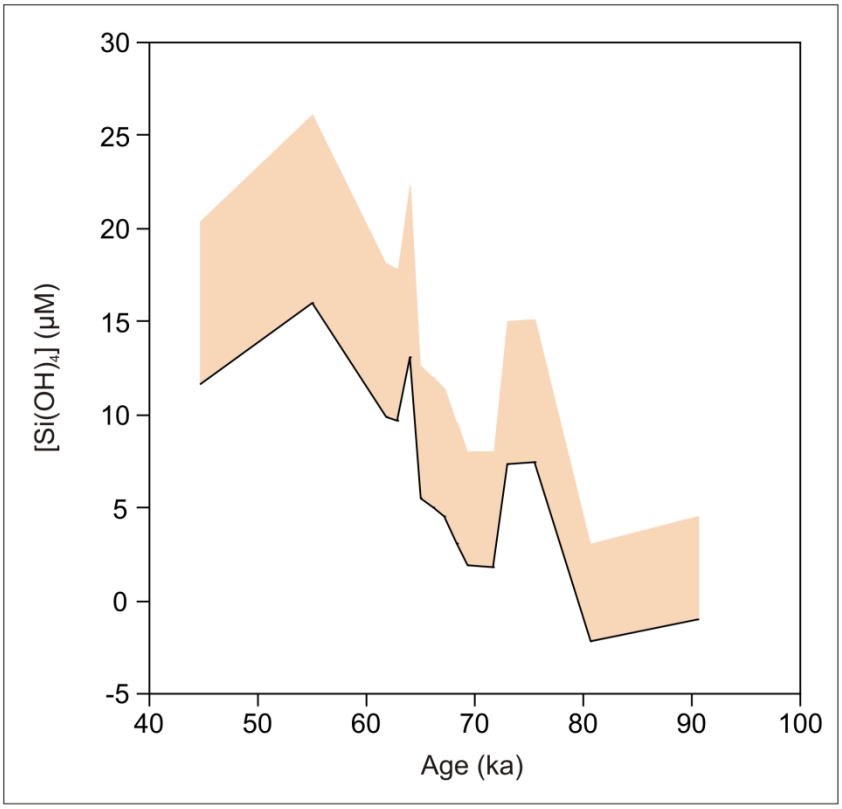

1063 Figure 7

1064

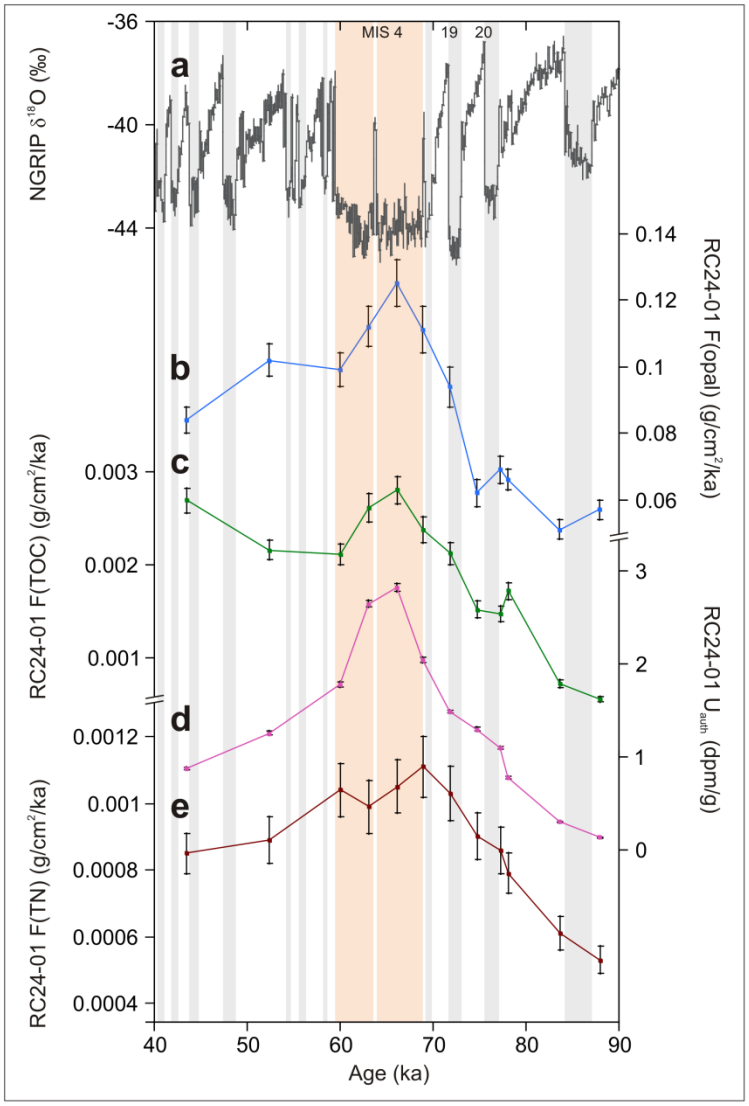

1065

1066

1067